

# Multivariable Backstepping and Adaptive LQ Control of Thermoacoustic Coupling in Jet Engine Systems

---

A Thesis  
Presented to  
the Faculty of the School of Engineering and Applied Science  
UNIVERSITY OF VIRGINIA

---

In Partial Fulfillment  
of the Requirements for the Degree  
Master of Science  
in  
Electrical Engineering

by  
Zackary Alexander Knoll

May 2015

APPROVAL SHEET

The thesis  
is submitted in partial fulfillment of the requirements  
for the degree of  
Master of Science

  
AUTHOR

The thesis has been read and approved by the examining committee:

Gang Tao  
\_\_\_\_\_  
Advisor

Zongli Lin  
\_\_\_\_\_

Scott Acton  
\_\_\_\_\_

\_\_\_\_\_

\_\_\_\_\_

\_\_\_\_\_

Accepted for the School of Engineering and Applied Science:



Dean, School of Engineering and Applied Science

May

2015

## Abstract

Jet engines are highly complex systems that have many internal processes which may become unstable under certain non-ideal conditions. These potentially unstable processes can induce instability in the overall engine process if left uncontrolled. One such process is known as thermoacoustic coupling. This is a process through which acoustic waves in the combustion chamber may become coupled with unsteady heat release at the flameholders, forming a positive feedback loop. Additionally, acoustic modes of close resonant frequency may become coupled and force the system to an unstable operating point. This process results in high amplitude pressure oscillations which in serious cases may result in permanent damage to the engine.

In this research, an indirect adaptive linear quadratic control scheme is first developed for a multi-input multi-output dynamic model of thermoacoustic coupling with unknown parameters and time delays. For this model, the controlling variable is the fuel mass flow into the combustion chamber. The time delays are modeled by a first-order Pade approximation. An adaptive controller design is developed to estimate the system and delay parameters, and an in-depth simulation study is conducted that verifies our results. The developed adaptive scheme has the ability to guarantee the desired stabilization properties in the presence of noisy inputs. When delays are large, it may not be appropriate to approximate time delays since it can introduce large errors into the system model. It is desirable to develop techniques that can directly handle large actuator delays. For this purpose, a nominal (non-adaptive) backstepping based actuator delay compensation scheme is derived and analyzed for systems in which time delays may be arbitrarily large. An extensive simulation study is also conducted to verify the developed backstepping delay control algorithm.

## Acknowledgements

I would like to thank Dr. Gary Dempsey, Dr. Jose Sanchez, and Mr. Nick Schmidt for their guidance and counseling through my undergraduate program. Your words of wisdom pushed me to extend my knowledge of engineering and always apply what I've learned to gain a better understanding.

I would also like to extend my gratitude to my graduate advisor, Dr. Gang Tao. If not for him, then I may not have been able to pursue a graduate degree at the University of Virginia. His encyclopedic knowledge of the subject has been an asset to my studies and his rigorous methods have taught me how to become a researcher in the field of control theory. I am grateful for the encouragement to start early and continue my research in a persistent manner, as it has eased stresses of my final push to complete my degree.

I would like to thank my colleagues Thummaros Rugthum, Korey Rankin, Cagatay Cebeci, and Zafer Vatansever for the useful feedback given and discussions had during my time here. These discussions have greatly deepened my knowledge and have been instrumental to the success of my research and studies. Additionally, I'd like to thank my girlfriend, Maggie, for the reassurance and help that she has given me during the last few months and for always finding a way to make me smile whenever I feel overwhelmed.

I am also very grateful to my parents, William and Annette, for their love and guidance. They have always pushed me to be the best that I can be, and taught me from an early age that my education is the most valuable thing that I can ever obtain. Thank you for the continuing reminder that, as long as I put my mind to it, I can achieve anything.

# Contents

<b>1</b>	<b>Introduction</b>	<b>1</b>
1.1	Literature Review . . . . .	2
1.2	Contributions . . . . .	4
1.3	Organization of Thesis . . . . .	5
<b>2</b>	<b>Background</b>	<b>6</b>
2.1	Adaptive Control Basics . . . . .	6
2.2	Indirect Adaptive Control Methodology . . . . .	8
2.3	Linear Quadratic Control Design . . . . .	12
2.4	Jet Engine Systems . . . . .	13
2.4.1	Operation and Engine Control Basics . . . . .	13
2.4.2	Thermoacoustic Coupling Model Derivation . . . . .	14
<b>3</b>	<b>Adaptive Controller Design with Delay Approximation</b>	<b>19</b>
3.1	Delay Approximation Model . . . . .	19
3.2	Nominal Controller Design . . . . .	23
3.3	Adaptive Linear Quadratic Control . . . . .	29
3.3.1	Control Design . . . . .	29
3.3.2	Parameter Estimation . . . . .	35
3.4	Simulation Study . . . . .	40
3.4.1	System Model . . . . .	40

---

3.4.2	Simulation Conditions and Cases . . . . .	42
3.4.3	Simulation Results for $Q = I$ . . . . .	44
3.4.4	Simulation Results for $Q = C_g^T C_g$ . . . . .	44
3.4.5	Simulation Results for Parameter Jump Case . . . . .	47
3.4.6	Simulation Results with Actuator Saturation . . . . .	52
<b>4</b>	<b>Backstepping Based Actuator Delay Compensation</b>	<b>55</b>
4.1	Delay Model . . . . .	56
4.2	Backstepping Transformation Design . . . . .	59
4.3	Stability Analysis . . . . .	67
4.4	Simulation Study . . . . .	72
4.4.1	Simulation Results . . . . .	73
<b>5</b>	<b>Conclusions and Future Work</b>	<b>77</b>
5.1	Conclusions . . . . .	77
5.2	Future Work . . . . .	78

# List of Figures

2.1	High level block diagram of a direct adaptive control system known as model reference adaptive control. . . . .	7
2.2	Diagram of a modern aircraft engine and operation [38]. . . . .	14
3.1	Block diagram of the adaptive LQ control system. . . . .	31
3.2	System outputs for $Q = I$ case with ideal controller (top), non-ideal controller (middle) and adaptive controller (bottom). . . . .	45
3.3	Control inputs for $Q = I$ case with ideal controller(top), non-ideal controller (middle), and adaptive controller (bottom). . . . .	45
3.4	Adaptive parameter estimates $\hat{\eta}, \hat{\zeta}, \hat{g}, \hat{f}$ for $Q = I$ case. . . . .	46
3.5	Output estimation error $\epsilon(t)$ for $Q = I$ case. . . . .	46
3.6	System outputs for $Q = C_g^T C_g$ case with ideal controller (top), non-ideal controller (middle) and adaptive controller (bottom). . . . .	47
3.7	Control inputs for $Q = C_g^T C_g$ case with ideal controller (top), non-ideal controller (middle) and adaptive controller (bottom). . . . .	48
3.8	Adaptive parameter estimates $\hat{\eta}, \hat{\zeta}, \hat{g}, \hat{f}$ for $Q = C_g^T C_g$ case. . . . .	48
3.9	Output estimation error $\epsilon(t)$ for $Q = C_g^T C_g$ case. . . . .	49
3.10	System outputs for the parameter jump case with ideal controller (top), non-ideal controller (middle) and adaptive controller (bottom). . . . .	50
3.11	Control inputs for the parameter jump case with ideal controller (top), non-ideal controller (middle) and adaptive controller (bottom). . . . .	50

---

3.12	Adaptive parameter estimates $\hat{\eta}, \hat{\zeta}, \hat{g}, \hat{f}$ for the parameter jump case. . .	51
3.13	Estimation error $\epsilon(t)$ for the parameter jump case. . . . .	51
3.14	System outputs for the parameter jump case with actuator saturation with ideal controller (top), non-ideal controller (middle) and adaptive controller (bottom). . . . .	53
3.15	Control inputs for the parameter jump case with actuator saturation with ideal controller (top), non-ideal controller (middle) and adaptive controller (bottom). . . . .	53
3.16	Adaptive parameter estimates $\hat{\eta}, \hat{\zeta}, \hat{g}, \hat{f}$ for the actuator saturation case.	54
3.17	Estimation error $\epsilon(t)$ for the with actuator saturation case. . . . .	54
4.1	System outputs for $\tau = 1$ case with actuator delay compensation. . .	74
4.2	Control inputs $u(t)$ for $\tau = 1$ case with actuator delay compensation.	74
4.3	System states for $\tau = 1$ case with ideal input (no compensation for actuator delay). . . . .	75
4.4	System outputs for $\tau = 3$ case with actuator delay compensation . . .	75
4.5	System states for $\tau = 3$ case with ideal input (no compensation for actuator delay). . . . .	76

# Chapter 1

## Introduction

In recent years, jet engine research has flourished. The literature has focused on topics such as reducing emissions while improving fuel efficiency, the development of advanced fault detection schemes, and the application of advanced control techniques for the engine system as a whole as well as the stabilization of certain unstable processes that may induce engine instability. Such unstable processes that may occur in the engine include compressor surge and stall, blade flutter, and thermoacoustic coupling, which will be our primary focus.

Thermoacoustic coupling is a phenomenon by which unsteady heat release may couple with the acoustics of the combustion chamber and lead to high amplitude pressure oscillations. In extreme cases, these uncontrolled pressure oscillations can lead to damage of the combustion chamber. This coupling has a few primary causes, the first of which being the use of a lean fuel-air mixture. This type of mixture is often used for reducing  $\text{NO}_x$  emissions as well as increasing the fuel efficiency of the engine. Aircraft contribute 1% of total mobile source  $\text{NO}_x$  emissions, and much higher percentages in city centers near major airports, so reducing emissions is a large concern [35],[36],[37]. While it is possible to passively control the resultant coupling of heat release and pressure waves through the physical design of the size and shape of the combustion chamber, it is more desirable to be able to operate the engine

over a wide range of operating conditions. Active control methods are frequently sought to perform this task. Additionally, it is possible for a situation to occur in which the fundamental properties of the engine may change, perhaps due to damage of some kind. In this case, the acoustics of the chamber may change and become more susceptible to perturbations, in which case, active control would be necessary for stabilization.

In addition to these problems, jet engines present difficult engineering challenges because of the incredibly harsh internal conditions. A result of this is difficulty in accurately determining the system parameters that are necessary for the design of traditional control systems. This motivates us to utilize adaptive parameter estimation techniques to update online estimates of the parameters needed to use an indirect adaptive control scheme. Additionally, since this system may also include uncertain time delays, we explore techniques that facilitate the use of adaptive parameter estimation to estimate these uncertain delays.

## 1.1 Literature Review

Jet engine control research spans a wide variety of areas. Some recent focuses and advancements include integrated flight/propulsion control [24]–[26], which incorporates advanced maneuvering capabilities such as vertical take off and landing and high-angle-of-attack performance into the control design, and intelligent life extending control where the focus is to minimize damage accumulation of components in the hot-gas-path over time [27]. Other research efforts include engine health monitoring and diagnostics [28]–[30], engine dynamic modeling for controls and diagnostics [32]–[34], and active combustion and stall control.

The potentially unstable processes mentioned previously have been long-standing

issues in jet engine control and design, as outlined in [16] and the many references therein. This thesis will focus on the specific case of thermoacoustic coupling. Suppression of thermoacoustic coupling has been demonstrated as a viable solution in both theory and practice. The paper in [7] along with its references detail a small portion of the extensive amount of theoretical and experimental work done on this topic. Experimental validation of active control was demonstrated on small-scale [12], mid-scale [13],[14], and large-scale/industrial [15] test rigs, showing that active control is a viable solution in practice as well as in theory. Some of the theoretical work can be seen in [8] where secondary peaks due to phase shifting controllers were explained and [9] where robust control was discussed. While the techniques implemented within these references are thorough, they do not consider the case where parameters are unknown. Various adaptive schemes have been implemented in [1], [10], and [11]; however these techniques do not satisfy the desired optimality in jet engine control.

In control design, time delays are often modeled by a Pade approximation which introduces system zeros that are non-minimum phase. Due to this, many direct adaptive control schemes such as MRAC techniques found in [4] and multivariable adaptive backstepping control [3] cannot be applied because the non-minimum phase zeros violate the design conditions. In addition, direct adaptive control schemes may lead to heavy overparameterization, which may cause difficulty in control implementation due to a lack of robustness. The adaptive control scheme that was designed in [1] uses an indirect adaptive pole placement scheme applicable to non-minimum phase systems; however, pole placement control often results in large transients in the control input. This motivates us to employ an adaptive linear quadratic control scheme, similar to that of [1] in using an indirect control design which estimates the system parameters and uses their online estimates to compute the control input, but different in that it is based on optimality design criterion helpful for reducing the

control magnitude.

When time delay approximation introduces large modeling errors that do not allow for the design of a sufficient controller, then control schemes that take the delays directly into account must be sought. Stability of time delay systems is much more difficult to examine than stability for standard LTI systems and a collection of techniques can be found in [44]. One method for control is known as the Smith predictor [39] and the extension to unstable plants derived in [40],[41],[42]. Recently, a new derivation of the Smith predictor was developed in [17], using a transport PDE model of actuator delay and a backstepping algorithm. This unique derivation allowed for the development of new adaptive control theory for systems with unknown time delays as was demonstrated in [19],[20],[21]. These references develop adaptive control theory for when actuator delays are unknown as well as having parameter uncertainties, estimated inputs, and nonlinear system structure, respectively.

## 1.2 Contributions

The model of thermoacoustic coupling that we use for control design contains unknown time delays in both the actuators and states. We utilize a first-order Pade approximation to model the delay terms. This modeling facilitates the development of an indirect adaptive linear quadratic control scheme for active control of thermoacoustic coupling. Such a control scheme also satisfies the desired optimality in jet engine systems. In some cases, it may be desirable to directly compensate for time delays instead of through an approximation. Because of this, another contribution of this thesis is the development of a novel backstepping algorithm for actuator delay compensation. The technique that this algorithm is based off of was recently demonstrated to be compatible with adaptive estimation of time delays [19],[20],[21]. Hence,

the development of this algorithm is the basis for future adaptive controls research for similar classes of delay differential equations.

### 1.3 Organization of Thesis

This thesis is organized as follows. Chapter 2 will discuss some fundamentals of adaptive control and linear quadratic control, then give a brief introduction to jet engines systems and operation, and discuss the modeling of the thermoacoustic coupling phenomenon. Chapter 3 will discuss our adaptive control scheme. This chapter briefly discusses modeling and delay approximation, presents a nominal controller design, and then extends the theory by presenting the adaptive controller design. Finally, an extensive simulation study is presented that verifies our design with non-ideal circumstances such as parameter jumps and actuator saturation. Chapter 4 develops a new backstepping algorithm that can be used with systems that have both state and actuator delays and provides a stability analysis and simulation study to verify the design.

# Chapter 2

## Background

The goal of this thesis is to develop reliable adaptive control schemes for unstable processes that may occur in jet engine systems that can induce instability such as thermoacoustic coupling, compressor surge and stall, and blade flutter. The focus of this section is to provide the necessary background for this thesis. We will begin by briefly recapping the basics of adaptive control. Then we will give a short discourse on indirect adaptive control methodology followed by a discussion of linear quadratic control. Finally, we present the basics of jet engine operation and control as well as a more in-depth discussion of the physics and modeling of the thermoacoustic coupling problem.

### 2.1 Adaptive Control Basics

All branches of control theory have the common goal of the manipulation of the system dynamics, which may include stabilization of an unstable plant, trajectory tracking, disturbance rejection and satisfying any desired performance specifications. Design of these systems typically requires that the engineer have a detailed mathematical model of the system where most, if not all, parameters are known. For more complex plants or those where certain system identification techniques are not feasible, it is

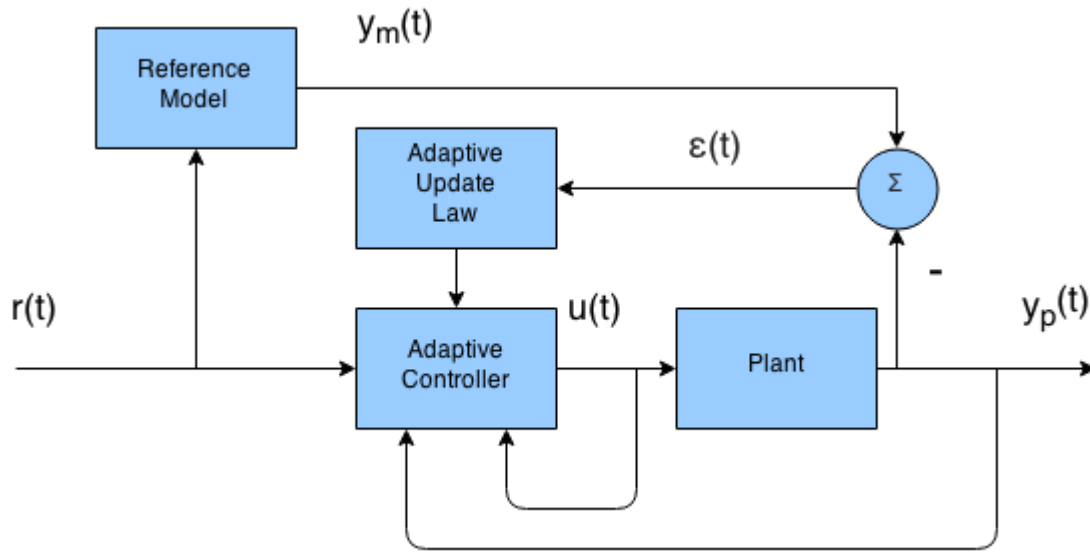


Figure 2.1: High level block diagram of a direct adaptive control system known as model reference adaptive control.

not possible to analytically design such controllers using the traditional techniques; furthermore, some system parameters may undergo change during operation. Under the initial conditions, a specific controller may be stabilizing; however, this same controller may no longer be stabilizing after this change has occurred. Adaptive control is the branch of control theory that is concerned with problems such as this.

Adaptive control design only requires knowledge of the basic system structure while parameters that govern the system may be unknown. The control gains are determined from an adaptive update law that is a function of the estimation error between expected and actual system signals. There are two primary techniques in adaptive control: direct adaptive control and indirect adaptive control. Direct adaptive control is the branch of adaptive control that produces on-line estimates of the controller gains, bypassing the need to determine the system parameters. Indirect adaptive control, in contrast, chooses to estimate the system parameters. These parameter estimates are then used to solve for the control input using a predetermined

control law. This will be the approach that we use in this paper. Fig. 2.1 shows a basic block diagram of an adaptive control system.

## 2.2 Indirect Adaptive Control Methodology

A typical indirect adaptive control scheme has two steps: estimation of the plant through the use of an adaptive law and the calculation of the control input from a predefined control law. One advantage that indirect adaptive control has over direct adaptive control schemes is that the numerator of the system transfer function is not required to be stable, meaning that the plant is allowed to have open-loop unstable zeros. Many direct adaptive schemes such as model reference adaptive control (MRAC) and adaptive backstepping are based on the assumption that all system poles are located in the left half of the complex plane.

To proceed with the adaptive estimation step, we require a parametric representation that defines a system in terms of a parameter vector and a vector of measurable signals. Consider the linear time-invariant plant

$$P(s)[y](t) = Z(s)[u](t) \quad (2.1)$$

where  $y(t) \in R$ ,  $u(t) \in R$  are the measured plant output and input, respectively. The polynomials  $Z(s)$ ,  $P(s)$  are of the form

$$\begin{aligned} P(s) &= s^n + p_{n-1}s^{n-1} + \cdots + p_1s + p_0 \\ Z(s) &= z_{m-1}s^{m-1} + z_{m-2}s^{m-2} + \cdots + z_1s + z_0. \end{aligned} \quad (2.2)$$

We begin by choosing an arbitrary stable polynomial  $\Lambda(s) = s^n + \lambda_{n-1}s^{n-1} + \cdots + \lambda_1s + \lambda_0$ . We then choose to filter both sides of equation (2.1) by the stable filter  $\frac{1}{\Lambda(s)}$

to obtain

$$\frac{1}{\Lambda(s)}P(s)[y](t) = \frac{1}{\Lambda(s)}Z(s)[u](t). \quad (2.3)$$

Manipulating this equation, we can obtain

$$y(t) = \frac{Z(s)}{\Lambda(s)}[u](t) + \frac{\Lambda(s) - P(s)}{\Lambda(s)}[y](t) \quad (2.4)$$

which can be expressed as

$$y(t) = \theta^{*T}\phi(t), t \geq 0 \quad (2.5)$$

where  $\theta^*$  is an unknown parameter vector, and  $\phi(t)$  is a vector of measurable signals.

These vectors are of the form

$$\theta^* = (z_0, z_1, \dots, z_{m-1}, z_m, \lambda_0 - p_0, \lambda_1 - p_1, \dots, \lambda_{n-2} - p_{n-2}, \lambda_{n-1} - p_{n-1})^T \in R^{n+m+1} \quad (2.6)$$

$$\phi(t) = \left( \frac{1}{\Lambda(s)}[u](t), \frac{s}{\Lambda(s)}[u](t), \dots, \frac{s^{m-1}}{\Lambda(s)}[u](t), \frac{s^m}{\Lambda(s)}[u](t), \frac{1}{\Lambda(s)}[y](t), \frac{s}{\Lambda(s)}[y](t), \dots, \frac{s^{n-2}}{\Lambda(s)}[y](t), \frac{s^{n-1}}{\Lambda(s)}[y](t) \right)^T \in R^{n+m+1}. \quad (2.7)$$

We can now define the estimation error as

$$\epsilon(t) = \theta^T(t)\phi(t) - y(t), t \geq t_0. \quad (2.8)$$

where  $\theta(t)$  is an estimate of the parameter vector  $\theta^*$ . Substituting equation (2.5) into this, we obtain

$$\epsilon(t) = \tilde{\theta}^T(t)\phi(t), \tilde{\theta}(t) = \theta(t) - \theta^*. \quad (2.9)$$

The representation given in (2.8) is a measurable signal and can be used in adaptation laws such as the normalized gradient algorithm or normalized least-squares algorithm.

For brevity and simplicity, only the gradient update law will be given as follows:

$$\dot{\theta} = -\frac{\Gamma\phi(t)\epsilon(t)}{m^2(t)}, \theta(t_0) = \theta_0. \quad (2.10)$$

Here,  $m(t)$  is a normalization signal that is generated to help guarantee stability properties and is of the form

$$m(t) = \sqrt{1 + \alpha\phi^T(t)\phi(t)}, \alpha > 0. \quad (2.11)$$

The parameter  $\Gamma = \Gamma^T > 0$  is an arbitrary gain matrix,  $\theta_0$  is an initial estimate of  $\theta^*$ , and  $\alpha > 0$  is a design parameter. Such a gradient parameter estimator guarantees the following properties that are useful in adaptive controller design:  $\theta(t), \dot{\theta}(t), \frac{\epsilon(t)}{m(t)}$  are bounded, and  $\dot{\theta}(t), \frac{\epsilon(t)}{m(t)} \in L^2$ .

The next step is to define a control law in terms of these parameter estimates. The control law that the designer uses will be heavily dependent upon the application and preference, but generally can be given as

$$u(t) = u(t; \theta(t), y(t), r(t)) \quad (2.12)$$

where  $r(t)$  may be a desired reference input for tracking. Techniques exist for adaptive pole placement control, adaptive model reference control, and adaptive LQ control, and each have their advantages and disadvantages. One potential pitfall of indirect adaptive control is that once the control law has been chosen, the current formulation cannot ensure that the given design equation always has a solution. This is known as the singularity problem. It is known that neither the gradient algorithm given above, nor the least-squares algorithm can ensure a singularity free adaptive controller. Therefore, the designer must study the system and then utilize robust

methods to ensure that the control law exists and is finite for all  $t \geq t_0$ .

One such robust method that can accomplish this is known as parameter projection. Given the unknown ideal parameter vector  $\theta^* \in R^{n+m+1}$ , then we assume that there exist known  $\theta_i^b > \theta^*$  and known  $\theta_i^a < \theta^*$  such that for the estimate  $\theta_i \in [\theta_i^a, \theta_i^b], i = 1, 2, \dots, n + m + 1$ , the control input  $u(t)$  exists and can be calculated from the estimate vector  $\theta(t)$  for  $t > t_0$ . To accomplish this, we choose the initial estimate  $\theta_i(0) \in [\theta_i^a, \theta_i^b]$  and define the adaptation signal as

$$g(t) = -\Gamma \frac{\phi(t)\epsilon(t)}{m^2(t)}. \quad (2.13)$$

From this, we obtain the projection signal as

$$f_i(t) = \begin{cases} 0 & \text{if } \theta_i(t) \in [\theta_i^a, \theta_i^b] \text{ or} \\ & \text{if } \theta_i(t) = \theta_i^a \text{ and } g_i(t) \geq 0 \text{ or} \\ & \text{if } \theta_i(t) = \theta_i^b \text{ and } g_i(t) \leq 0 \\ -g_i(t) & \text{otherwise} \end{cases}. \quad (2.14)$$

The projection vector is then built as  $f(t) = [f_1(t), f_2(t), \dots, f_{n+m+1}(t)]$ . From this we define the new parameter update law as

$$\dot{\theta} = -\Gamma \frac{\phi(t)\epsilon(t)}{m^2(t)} + f(t). \quad (2.15)$$

This choice of  $f(t)$  ensures that  $\theta_i(t) \in [\theta_i^a, \theta_i^b], i = 1, 2, \dots, n + m + 1$  for all time by negating the adaptation signal if it were to move outside of the specified interval. Thus, the parameter projection method can ensure that the control law  $u(t)$  exists and is finite when the estimate vector  $\theta(t)$  is used to calculate it. It can also be shown that the parameter projection operator does not harm the ideal properties of

boundedness and finite energy given by the gradient parameter estimator.

## 2.3 Linear Quadratic Control Design

A branch of control theory known as optimal control deals with the determination of control laws through mathematical optimization. The design problem is defined in terms of a cost function that is comprised of the state and control variables. The optimal control is the path that the control variables must take in order to minimize the cost function. A special case of general optimal control is known as the linear quadratic control problem. Given the LTI system described by

$$\dot{x} = Ax(t) + Bu(t), \quad (2.16)$$

the LQ control problem is given as the minimization of the cost function

$$J = \int_0^{\infty} \left[ x^T(t)Qx(t) + u^T(t)Ru(t) \right] dt \quad (2.17)$$

where  $Q = Q^T \geq 0, R = R^T > 0$  are cost matrices. The LTI system state equations act as the set of linear constraints for the cost function, completing the mathematical formulation of the optimization problem. The goal of this problem is to determine the optimal state feedback

$$u(t) = -Kx(t) \quad (2.18)$$

$$K = R^{-1}B^TP \quad (2.19)$$

that will minimize (2.17).  $K$  is the optimal gain matrix and depends on a  $P = P^T \geq 0$  that is the solution to the algebraic Riccati equation

$$A^T P + PA - PBR^{-1}B^T P + Q = 0. \quad (2.20)$$

The solution  $P$  is known to exist, given the restriction that the pair  $(A, B)$  is controllable. The resultant gain matrix  $K$  will generate a stabilizing control law for the system in (2.16) and is optimal in the sense of the cost function (2.17).

## 2.4 Jet Engine Systems

This section will present some basics of jet engine systems that will be relevant to the rest of the thesis. We begin with engine operation and function and then discuss the role of control systems in jet engines. We then give a summary of the modeling of the thermoacoustic coupling phenomenon. This modeling includes the physics-based distributed model and derives a reduced model that is useful for control design.

### 2.4.1 Operation and Engine Control Basics

In general, a jet engine system refers to any air-breathing, internal combustion engine that generates thrust via the discharge of a fast moving jet. Modern aircraft engines are the most prevalent of such engines and are the focus of this thesis. Figure 2.2 depicts a typical aircraft engine known as a turbojet and its standard gas flow paths. As can be seen, air enters the engine at the front intake and is passed through a set of axial and/or centrifugal compressors. Typically the engine is either a single-spool or multi-spool engine, having either one or multiple compressor and fan combinations. The compressed air is then mixed with fuel at the entrance to the combustion chamber

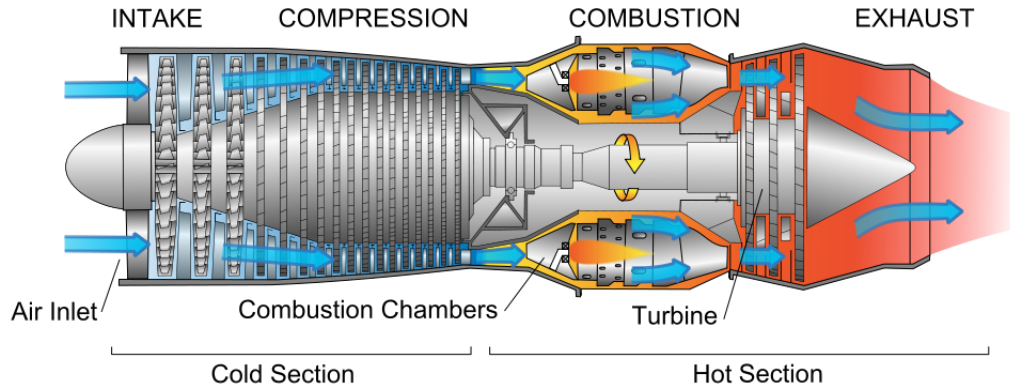


Figure 2.2: Diagram of a modern aircraft engine and operation [38].

and ignited. The resulting hot gases are ejected in a jet out of the exhaust that produces thrust.

As these engines are highly nonlinear, a typical jet engine control system contains several feedback loops that control various engine processes with the common goal of maintaining a desired operating condition over time. At this operating point, the primary engine control loop will typically take the pilot's power request as an input, convert this to either shaft speed or engine pressure ratio (as these signals typically correlate well with thrust), and compute the desired fuel flow rate. The loop is then closed by sensing the shaft speed or pressure ratio and feeding it back.

### 2.4.2 Thermoacoustic Coupling Model Derivation

Thermoacoustic coupling is one example of an internal process that can be controlled in order to maintain stable operation of the engine at a desired operating point. This phenomenon occurs as a result of unsteady heat release in the combustion chamber. This heat release excites acoustic waves which, in turn, perturb the fuel-air mixture entering the chamber. If this perturbation is strong enough, resonant pressure modes may become unstable. This instability results in high amplitude pressure oscillations

which, in extreme cases, can lead to damage or reduced lifetime of the combustion chamber. In addition, resonant modes of close resonant frequency may become coupled which may further decrease stability. This motivates the development of a multivariable model for the control of this process. The references [1] and [2] develop this model from the linear distributed thermoacoustic model

$$\frac{\partial}{\partial t} \tilde{p}(x, y, z, t) + \bar{u}(x, y, z) \cdot \nabla \tilde{p}(x, y, z, t) + \Delta \phi(x, y, z, t) = \tilde{q}(x, y, z, t) \quad (2.21)$$

$$\frac{\partial}{\partial t} \phi(x, y, z, t) + \bar{u}(x, y, z) \cdot \nabla \phi(x, y, z, t) + a^2 \tilde{p}(x, y, z, t) = \eta(x, y, z, t) \quad (2.22)$$

$$\frac{\partial}{\partial t} y_f(x, y, z, t) + \bar{u}(x, y, z) \cdot \nabla y_f(x, y, z, t) = 0 \quad (2.23)$$

$$\tilde{q}(x, y, z, t) = F'_{hr}(\bar{Y}_f(x, y, z)) \gamma_{flame}(x - g_{fl}(y, z)) y_f(x, y, z, t) \quad (2.24)$$

where  $\tilde{p}, \tilde{q}$  are the normalized pressure and heat release perturbations, respectively,  $\phi, \eta$  are the velocity and noise potential,  $\bar{u}, u'$  are the mean and perturbation velocity of the fuel-air mixture, and  $g_{fl}(y, z)$  represents the fixed flame surface. The mean fuel mass fraction  $\bar{Y}_f(x_0, y, z)$ , perturbation fuel mass fraction  $y_f(x_0, y, z, t)$ , and axial and local heat release functions  $\gamma_{flame}(\cdot), F'_{hr}(\cdot)$  are defined in depth in the source material. This distributed model is not convenient for control design, so a reduced order model is introduced. The first step is to expand the pressure and potential perturbations in terms of the acoustic resonant modes. This results in

$$\tilde{p}(x, t) = \sum_{i=1}^n y_i(t) \Pi_i(x) \quad (2.25)$$

and

$$\phi(x, t) = \sum_{i=1}^n \phi_i(t) \Pi_i(x). \quad (2.26)$$

where  $\Pi_i(x)$  are spatial resonant mode shapes, and  $y_i(t)$  and  $\phi_i(t)$  govern how the pressure and potential mode shapes fluctuate in time. As is commonly done, we now apply a Galerkin approximation [1], [2], [8] to obtain

$$j\omega \begin{bmatrix} \Phi_1(j\omega) \\ \Phi_2(j\omega) \\ Y_1(j\omega) \\ Y_2(j\omega) \end{bmatrix} = \begin{bmatrix} 0 & 0 & -a^2 & 0 \\ 0 & 0 & 0 & -a^2 \\ \lambda_1 & 0 & 0 & 0 \\ 0 & \lambda_2 & 0 & 0 \end{bmatrix} \begin{bmatrix} \Phi_1(j\omega) \\ \Phi_2(j\omega) \\ Y_1(j\omega) \\ Y_2(j\omega) \end{bmatrix} + \begin{bmatrix} N_1(j\omega) \\ N_2(j\omega) \\ Q_1(j\omega) - V_1(j\omega) \\ Q_2(j\omega) - V_2(j\omega) \end{bmatrix}, \quad (2.27)$$

where  $Y_m(j\omega)$  is the Fourier transform of  $y_m(t)$ ,  $\Phi_m(j\omega)$  is the Fourier transform of  $\phi_m(t)$ , and  $Q_m(j\omega)$ ,  $N_m(j\omega)$ , and  $V_m(j\omega)$  are the Fourier transforms of

$$q_m(t) = \int_{\mathcal{V}} \Pi_m(x) \tilde{q}(x, t) dx \quad (2.28)$$

$$\eta_m(t) = \int_{\mathcal{V}} \Pi_m(x) \tilde{\eta}(x, t) dx \quad (2.29)$$

$$v_m(t) = \int_{\mathcal{S}} \Pi_m(x) u'_n(x, t) dx \quad (2.30)$$

respectively. Here,  $\mathcal{V}$  and  $\mathcal{S}$  represent the combustion chamber volume and surface, and the coefficient  $\lambda_m > 0$  is defined as

$$\lambda_m = \frac{\int_{\mathcal{V}} |\nabla \Pi_m(x)|^2 dx}{\int_{\mathcal{V}} |\Pi_m(x)|^2 dx}. \quad (2.31)$$

Equation (2.27) can be simplified to obtain the expression

$$((j\omega)^2 + \lambda_k a^2) Y_k(j\omega) = (j\omega)(Q_k(j\omega) - V_k(j\omega)) + \lambda_k N_k(j\omega), \quad k = 1, 2 \quad (2.32)$$

and the functions  $V_m(j\omega)$ ,  $Q_m(j\omega)$  are given as

$$V_m(j\omega) = G_m^{bc}(j\omega)Y_m(j\omega) \quad (2.33)$$

$$Q_m(j\omega) = \sum_{k=1}^2 G_{mk}^{p2q}(j\omega)Y_m(j\omega) + \sum_{i=1}^{N_{inj}} G_{mi}^{uf2q}(j\omega)W_{f,i}(j\omega). \quad (2.34)$$

where transfer functions  $G_m^{bc}(j\omega)$ ,  $G_{mk}^{p2q}(j\omega)$ ,  $G_{mi}^{uf2q}(j\omega)$  are defined in [1] and [2]. Substituting equations (2.33) and (2.34) into (2.32) we obtain

$$\begin{aligned} & ((j\omega)^2 + (j\omega)G_k^{bc}(j\omega) + \lambda_k a^2)Y_k(j\omega) \\ &= \sum_{m=1}^2 (j\omega)G_{km}^{p2q}Y_m(j\omega) + \sum_{i=1}^{N_{inj}} G_{mi}^{uf2q}(j\omega)(j\omega)W_{f,i}(j\omega) + \lambda_k N_k(j\omega), \quad k = 1, 2. \end{aligned} \quad (2.35)$$

We now make some simplifying assumptions regarding the remaining transfer functions. The first is that the boundary admittance is a real positive number such that

$$G_k^{bc}(j\omega) = \xi_{kk}, \quad (2.36)$$

which is valid as acoustic boundary conditions are designed to maximize the real part of admittance for optimal acoustic damping. The second assumption proposes that the distributed delays contained in the heat release transfer functions can be represented as a real positive number and a lumped delay term. That is,

$$G_{kk}^{uf2q}(j\omega) \approx g_{kk} e^{j\omega\tau_{c,k}} \quad (2.37)$$

$$(j\omega)G_{km}^{p2q}(j\omega) \approx -\zeta_{km} e^{j\omega\tau_{km}}. \quad (2.38)$$

This is based on the assumption that in a narrow band around the resonant frequency, any transfer function with flat magnitude response and rolling off phase response can be approximated as a lumped delay and static gain. With this, equation (2.35) results in a set of delay differential equations of the form

$$\begin{aligned} \ddot{y}_1 + \xi_{11}\dot{y}_1 + \eta_{11}y_1 + \zeta_{11}y_1(t - \tau_{11}) + \zeta_{12}y_2(t - \tau_{12}) &= g_{11}\dot{u}_2(t - \tau_{c,1}) + h_{11}\chi_1 \\ \ddot{y}_2 + \xi_{22}\dot{y}_2 + \eta_{22}y_2 + \zeta_{22}y_2(t - \tau_{22}) + \zeta_{21}y_1(t - \tau_{21}) &= g_{22}\dot{u}_1(t - \tau_{c,2}) + h_{22}\chi_2. \end{aligned} \quad (2.39)$$

For this specific case of coupling, we can take advantage of the circular symmetry of the combustion chamber and the fact that for the two pressure modes, one is obtained by a 90 degree rotation of the other. These two properties of the application result in the above model reducing to

$$\begin{aligned} \ddot{y}_1 + \eta y_1 + \zeta y_2(t - \tau) &= g\dot{u}_2(t - \tau) + h\chi_1 \\ \ddot{y}_2 + \eta y_2 - \zeta y_1(t - \tau) &= -g\dot{u}_1(t - \tau) + h\chi_2. \end{aligned} \quad (2.40)$$

This is the model that we base our control system design off of. The next chapter will develop an indirect adaptive control scheme for when it is appropriate to estimate the lumped delay  $\tau$  and provide simulation results verifying our design. Then, the following chapter will examine a novel technique for control of the delay system without approximations.

# Chapter 3

## Adaptive Controller Design with Delay Approximation

The following sections will present the design case where all system parameters, including time delays, are unknown, and the delays are estimated using a first-order Pade approximation. This thesis applies techniques of optimal control theory, namely linear quadratic control, to stabilize the simplified jet engine instability model that is used to describe thermoacoustic coupling. We will begin by modeling the physical system in state space with approximated time delays. Following this, we will solve the control problem for the nominal case where all system parameters are known. We will then approach the adaptive control problem using an indirect adaptive scheme, as the more common direct adaptive schemes require the assumption that all system zeros be stable. We end by presenting the simulation results that verify our design.

### 3.1 Delay Approximation Model

For a complex system such as a jet engine, it is possible that the system time delays may be unknown which makes the control problem significantly harder. A technique that may be used in situations where the time delay is sufficiently small compared

to the system dynamics is to use a simple approximation such as a first-order Pade approximation. The benefit of this approximation is that it allows us to transform a functional differential equation - one that includes time delays - into an ordinary differential equation system. Furthermore, if the time delay is unknown, then the approximation allows for the use of existing adaptive control techniques for estimation. It is known that for an arbitrary delayed signal  $f(t)$ ,

$$\mathcal{L}[f(t - \tau)] = \mathcal{L}[f(t)]e^{-\tau s} \quad (3.1)$$

where  $\mathcal{L}[\cdot]$  is the Laplace transform operator. From this, we can obtain the first-order approximation of a time delayed signal as

$$e^{\frac{-2s}{f}} \approx \frac{f - s}{f + s}, \tau = \frac{2}{f}. \quad (3.2)$$

Such an approximation allows for the derivation of a model that is suitable for control design.

Taking the Laplace transform of the model in (2.40) and applying the approximation in equation (3.2), we obtain the equations

$$\begin{aligned} (s^2 + \eta)Y_1 + \zeta Y_2 \frac{f - s}{f + s} &= gsU_2 \frac{f - s}{f + s} + hX_1 \\ (s^2 + \eta)Y_2 - \zeta Y_1 \frac{f - s}{f + s} &= -gsU_1 \frac{f - s}{f + s} + hX_2 \end{aligned} \quad (3.3)$$

where  $Y_i$ ,  $U_i$ , and  $X_i$  are the Laplace transforms of the signals  $y_i$ ,  $u_i$ , and  $\chi_i$  for  $i = 1, 2$ .

Define the matrices  $P_1, Q_1$  as

$$Q_1 = \eta I + \zeta P_1,$$

$$P_1 = \begin{bmatrix} 0 & 1 \\ -1 & 0 \end{bmatrix}.$$

Simplifying the above equations we obtain

$$\begin{aligned} (s^3 + fs^2\eta s + f\eta)Y_1 + \zeta Y_2(f - s) &= gsU_2(f - s) + h(f + s)X_1 \\ (s^3 + fs^2\eta s + f\eta)Y_2 - \zeta Y_1(f - s) &= -gsU_2(f - s) + h(f + s)X_2 \end{aligned} \quad (3.4)$$

which can be combined into matrix form as

$$(Is^3 + fIs^2 + Q_1s + fQ_1)[y](t) = g(f - s)sP_1[u](t) + h(s + f)I\chi \quad (3.5)$$

where  $y = [y_1, y_2], u = [u_1, u_2]$  are the output and input vectors, and  $\chi = [\chi_1, \chi_2]$  is the disturbance input vector. The parameters  $f, g, h, \eta, \zeta$  are all unknown system parameters. This system is in a standard MIMO form

$$\begin{aligned} A(s)y &= B(s)u + C(s)\chi \\ A(s) &= (Is^3 + fIs^2 + Q_1s + fQ_1) \\ B(s) &= g(f - s)sP_1 \\ C(s) &= h(s + f)I. \end{aligned} \quad (3.6)$$

According to [4], a MIMO system represented in the above form, and

$$A(s) = Is^n + A_{n-1}s^{n-1} + \dots + A_1s + A_0 \quad (3.7)$$

$$B(s) = B_{n-1}s^{n-1} + B_{n-2}s^{n-2} + \dots + B_1s + B_0 \quad (3.8)$$

can be represented in a MIMO observer canonical form given as

$$\begin{aligned} \dot{x} &= A_o x + B_o u \\ y &= C_o x \end{aligned} \quad (3.9)$$

where

$$A_o = \begin{bmatrix} A_{n-1} & I & 0 & \dots & 0 \\ A_{n-2} & 0 & I & \dots & 0 \\ \vdots & \vdots & \vdots & \ddots & \vdots \\ A_1 & 0 & 0 & \dots & I \\ A_0 & 0 & 0 & 0 & 0 \end{bmatrix}, B_o = \begin{bmatrix} B_{n-1} \\ B_{n-2} \\ \vdots \\ B_0 \end{bmatrix} \quad (3.10)$$

and

$$C_o = \begin{bmatrix} I & 0 & \dots & 0 & 0 \end{bmatrix}. \quad (3.11)$$

We can put equations (3.5)–(3.6) into the MIMO observer canonical form where the state equations are of the form

$$\begin{aligned} \dot{x} &= A_g x + B_g u + D_g \chi, \quad x \in R^6 \\ y &= C_g x \end{aligned} \quad (3.12)$$

where  $A_g, B_g, D_g$  are formed as

$$A_g = \begin{bmatrix} -fI & I & 0 \\ -Q_1^T & 0 & I \\ -fQ_1 & 0 & 0 \end{bmatrix}, B_g = \begin{bmatrix} -gP_1 \\ gfP_1 \\ 0 \end{bmatrix}, D_g = \begin{bmatrix} 0 \\ hI \\ hfI \end{bmatrix}. \quad (3.13)$$

In this form, the output matrix  $C_g$  is known, and it is given as

$$C_g = \begin{bmatrix} I & 0 & 0 \end{bmatrix}. \quad (3.14)$$

## 3.2 Nominal Controller Design

In optimal control, the motivation is to construct a control law that will minimize a given cost function. The cost function is determined according to the system specifications so that the designer can place high or low costs on certain deviations. The magnitude of the control input is included in the cost function in order to limit the energy expended by it, as large values of the control input are often undesirable because of the potential for actuator saturation. For linear quadratic control, the control objective is to choose an optimal state feedback controller for the generic system

$$\begin{aligned} \dot{x} &= Ax + Bu, \quad x \in R^n, \quad u \in R^m \\ y &= Cx \end{aligned} \quad (3.15)$$

subject to the cost function

$$J = \int_0^{\infty} (x^T Q x + u^T R u) dt \quad (3.16)$$

where  $Q = Q^T \in R^{n \times n}$  is a positive semidefinite matrix and  $R = R^T \in R^{m \times m}$  is a positive definite matrix, chosen to meet certain optimality. In particular,  $R$  and  $Q$  can be treated as the weighting factors for the cost specification on  $x$  and  $u$  in  $J$  to be minimized.

For adaptive LQ control when the system matrices  $A$ ,  $B$  and  $C$  are unknown, we

choose  $Q = C^T C$  so that  $x^T Q x = y^T y$ , leading to certain optimality specification on the system output  $y(t)$ , and with  $u^T R u$ , on  $u(t)$ , relatively. Then an input-output system model can be employed for the construction of an adaptive observer (see next subsection).

To achieve our goals of stabilization and minimization of  $J$ , we will utilize an optimal control theory to generate the control law. A summary of linear quadratic control can be found in Section 2.3 and in [5]. We will discuss the nominal control cases for the known system parameter case first, as the basis for an adaptive control design for the unknown parameter case.

We begin our controller design by deriving the nominal controller when all system parameters and matrices are known. We will look at two approaches in order to build the theory: the first being state feedback control when all system states are measurable, and the second being observer-based feedback control for the case when we may have arbitrary unmeasurable states.

### State Feedback Control Design

When all states of the open loop system are available for measurement, an effective controller is a state feedback controller. The cost function (3.16) can be minimized by using the control law

$$\begin{aligned} u &= -Kx \\ K &= R^{-1}B^T P \end{aligned} \tag{3.17}$$

where  $P \in R^{n \times n}$  is a positive definite matrix satisfying the Riccati Equation

$$A^T P + PA - PBR^{-1}B^T P + Q = 0. \tag{3.18}$$

To ensure the existence of such a matrix  $P$  and a minimal value of  $J$ , for a feasible LQ control design, we need the following condition:

**(A1)** The pair  $(A, B)$  is stabilizable (to ensure that a finite cost function  $J$  is possible by making the closed-loop stable, so that a minimal  $J$  can be found), and the pair  $(A, C_0)$  is observable for  $C_0 \in R^{p \times n}$  being such that  $Q = C_0^T C_0$  (to ensure that a finite (minimal)  $J$  leads to  $\lim_{t \rightarrow \infty} x(t) = 0$  so that the closed-loop system is asymptotically stable—it is sufficient for this if  $(A, C_0)$  is detectable—and to ensure the existence of a unique  $P = P^T > 0$  to the Riccati equation—a detectable  $(A, C_0)$  can only ensure a unique solution  $P = P^T \geq 0$ ).

The optimal controller (3.17) can be directly applied to the system (3.12) with  $\chi = 0$  if  $x(t)$  is available for measurement. The matrix  $Q$  can be chosen as  $Q = C_g^T C_g$  as  $(A_g, C_g)$  is observable. The control law results in the closed-loop state equation

$$\dot{x} = (A_g - B_g R^{-1} B_g^T P)x. \quad (3.19)$$

Given that  $(A_g, B_g)$  is stabilizable and  $Q$  and  $R$  are chosen as positive semidefinite and positive definite, respectively, a  $P = P^T > 0$  exists and is a unique solution to the Riccati Equation (3.18). It will result in all eigenvalues of the closed-loop system matrix  $(A_g - B_g K)$  having negative real parts. This control law also guarantees boundedness of all closed-loop signals and  $y(t) \rightarrow 0$  exponentially fast.

### Observer-Based Feedback Control Law

In general, the system state variables  $x(t)$  may not be available for measurement, so in order to use a state feedback based control scheme such as linear quadratic control, we will make use of a state observer for the system in (3.12) (which is a special form

of (3.15)) of the form

$$\dot{\hat{x}} = A_g \hat{x} + B_g u - K_o(C_g \hat{x} - y) \quad (3.20)$$

where the observer gain  $K_o \in R^{6 \times 2}$  is chosen to meet the matching equation

$$\det(sI - A_g + K_o C_g) = A_o^*(s) \quad (3.21)$$

for a desired  $n$ th-order monic and stable polynomial  $A_o^*(s)$ , which can be realized under the observability condition of  $(A_g, C_g)$ .

Then, the observer-based control law that minimizes the cost function (3.16) is given by

$$u = -K \hat{x}, \quad (3.22)$$

$$K = R^{-1} B_g^T P \quad (3.23)$$

where  $P \in R^{n \times n}$  is a positive definite matrix satisfying the Riccati Equation

$$A_g^T P + P A_g - P B_g R^{-1} B_g^T P + Q = 0. \quad (3.24)$$

To ensure the existence of such a matrix  $P$  and a minimal value of  $J$ , for a feasible LQ control design we require assumption (A1) to hold, with  $A = A_g, B = B_g, C_0 = C_g$  for the  $(A_g, B_g, C_g)$  given in (3.13).

In order to properly utilize the state observer, the designer should choose the poles of the observer to be sufficiently fast so that the state estimates converge much faster than their respective states. Since the observer is stable by design, then under the assumptions of stabilizability and with the additional assumption of observability, then we can guarantee the boundedness of all closed-loop signals and  $\lim_{t \rightarrow \infty} \hat{x}(t) =$

$x(t)$  exponentially fast. In turn, this will lead to the conclusion that  $\lim_{t \rightarrow \infty} y(t) = 0$ .

### Existence of Solution

The Riccati equation in 3.24 requires two conditions to guarantee the existence of a finite, unique solution. The first condition is that  $R = R^T > 0$ , and  $Q = Q^T \geq 0$ , and are chosen by the designer. The second condition is that the matrix pair  $(A_g, B_g)$  is stabilizable. To guarantee this condition we must examine the controllability of the system (3.12).

Controllability for the matrix pair  $(A_g, B_g)$  is given by the equation

$$\mathcal{C} = [B_g \ A_g B_g \ A_g^2 B_g \ A_g^3 B_g \ A_g^4 B_g \ A_g^5 B_g] \quad (3.25)$$

The matrix  $\mathcal{C}$  must be of full rank to ensure controllability. While for a 6th order system, examining this matrix is cumbersome, we will examine a submatrix that will also give us insight into the controllability of the system. Consider the submatrix

$$\mathcal{C}_3 = [B_g \ A_g B_g \ A_g^2 B_g]. \quad (3.26)$$

Expanding this matrix results in

$$\mathcal{C}_3 = \begin{bmatrix} 0 & -g & 0 & 2fg & g\zeta & g(\eta - 2f^2) \\ g & 0 & -2fg & 0 & -g(\eta - 2f^2) & g\zeta \\ 0 & fg & g\zeta & g\eta & -3fg\zeta & -fg\eta \\ -fg & 0 & -g\eta & g\zeta & fg\eta & -3fg\zeta \\ 0 & 0 & -fg\zeta & fg\eta & 2f^2g\zeta & -2f^2g\eta \\ 0 & 0 & -fg\eta & -fg\zeta & 2f^2g\eta & 2f^2g\zeta \end{bmatrix}. \quad (3.27)$$

If  $\text{rank}[\mathcal{C}_3] = 6$  then we will know that the controllability matrix  $\mathcal{C}$  has full rank, thus implying the system is controllable. Since  $\mathcal{C}_3$  is a square matrix, full rank implies that the matrix is nonsingular, so we take the determinant as follows:

$$\begin{aligned} \det \mathcal{C}_3 &= 4f^4g^6\eta^4 + 8f^6g^6\eta^3 + 4f^8g^6\eta^2 + 4f^4g^6\eta^2\zeta^2 + 8f^6g^6\eta\zeta^2 + 4f^8g^6\zeta^2 \\ &= 4f^4g^6(\eta^4 + 2f^2\eta^3 + f^4\eta^2 + \eta^2\zeta^2 + 2f^2\eta\zeta^2 + f^4\zeta^2) \end{aligned} \quad (3.28)$$

This yields a set of necessary conditions that guarantee the controllability of the system (3.12). These are as follows

- (C1)  $f \neq 0$
- (C2)  $g \neq 0$
- (C3)  $\eta \neq \zeta \neq 0$
- (C4)  $\eta^4 + f^4\eta^2 + \eta^2\zeta^2 + f^4\zeta^2 \neq -2f^2\eta^3 - 2f^2\eta\zeta^2$

For us to reasonably assume that our system is controllable, we must examine each of these conditions. Condition (C1) is reasonable to assume true since  $f = 0$  would imply that the time delay  $\tau$  is infinite. The next condition, (C2), is reasonable to assume because  $g = 0$  would imply that we have zero control authority, which is simply not true. (C3) is a reasonable assumption because  $\zeta = 0$  would imply that there is zero coupling between the acoustic modes. We are specifically looking at the case where there is a strong coupling between modes. Additionally, if  $\eta = 0$  then the original differential equation would only depend on the input, which we know to be not true. The last condition, (C4), is more complex; however, we see that an inclusive requirement of (C4) is that  $\eta < 0$ . From [1] and [2], we know that this term is related to the acoustic resonant frequency, so it must be greater than zero. With  $\eta > 0$  condition (C4) will always be satisfied.

### 3.3 Adaptive Linear Quadratic Control

Jet engines are highly complex systems. Due to the system nature, poorly understood physical phenomena, and time-varying parameters, obtaining accurate parameter values is difficult. Thus, we consider the case in which system parameters  $f, g, \eta, \zeta$  are unknown. Adaptive control is an effective tool in such cases due to its ability to obtain online parameter estimates and update them during operation. As stated previously, the first-order Pade approximation results in a non-minimum phase realization of the model in (2.40). This, along with the desired optimality for jet engines, motivates us to utilize an indirect adaptive linear quadratic control scheme. We begin with the controller design, discuss the reduced-order parameter estimation and robust adaptive laws, and then present a detailed simulation study to verify our results.

#### 3.3.1 Control Design

Since the parameters  $A_g$  and  $B_g$  of

$$\dot{x} = A_g x + B_g u, \quad y = C_g x \quad (3.29)$$

are unknown, we use the adaptive version of the control law (3.22) as

$$u = -\hat{K}\hat{x}, \quad \hat{K} = R^{-1}\hat{B}_g^T(t)P(t) \quad (3.30)$$

where  $P(t)$  is the solution of the online Riccati equation

$$\hat{A}_g^T P(t) + P(t)\hat{A}_g - P(t)\hat{B}_g R^{-1}\hat{B}_g^T P(t) + Q = 0. \quad (3.31)$$

$\hat{A}_g$  and  $\hat{B}_g$  are adaptive estimates of  $A_g$  and  $B_g$ , and  $\hat{x}$  is produced by the adaptive observer

$$\dot{\hat{x}} = \hat{A}_g \hat{x} + \hat{B}_g u - \hat{K}_o (C_g \hat{x} - y), \quad (3.32)$$

with  $\hat{K}_o \in R^{6 \times 2}$  chosen to satisfy

$$\det(sI - \hat{A}_g + \hat{K}_o C_g) = A_o^*(s). \quad (3.33)$$

The implementation of this indirect adaptive control scheme requires that our estimates of the system matrices  $\hat{A}_g$  and  $\hat{B}_g$  satisfy some crucial conditions.

**(A2):** The estimates  $\hat{A}_g(t)$  and  $\hat{B}_g(t)$  are such that  $\hat{A}_g(t), \hat{B}_g(t) \in L^\infty$  and  $\dot{\hat{A}}_g(t), \dot{\hat{B}}_g(t) \in L^2$ , plus some desired estimation error conditions (see Section 3.3.2).

Also, in order to utilize parameter projection and form the projection signal, we will require some basic knowledge of our system parameters.

**(A3):** The parameters  $f, g, \eta, \zeta$  satisfy  $|f| \geq f_0 > 0$ ,  $|g| \geq g_0 > 0$ ,  $|\eta| \geq \eta_0 > 0$ ,  $|\zeta| \geq \zeta_0 > 0, \forall t \geq 0$  for some known lower bounds  $f_0, g_0, \eta_0, \zeta_0$  and  $\text{sign}[f]$ ,  $\text{sign}[g]$ ,  $\text{sign}[\eta]$ ,  $\text{sign}[\zeta]$  are known.

The assumption (A3) allows the implementation of parameter projection for robust control. The use of parameter projection will allow us to manipulate the adaptive law so that we can guarantee that a solution to the online Riccati equation in (3.31) always exists, as we will discuss next. An overall block diagram for the adaptive control system is seen in Fig. 3.1.

**Controllability and Observability.** The adaptive Riccati equation given in (3.31) requires two conditions to guarantee the existence of a finite, unique solution. The first condition is that the matrices  $R = R^T > 0$  and  $Q = Q^T \geq 0$ , which are chosen by the designer. The second condition is that at any frozen time  $t > 0$ , the

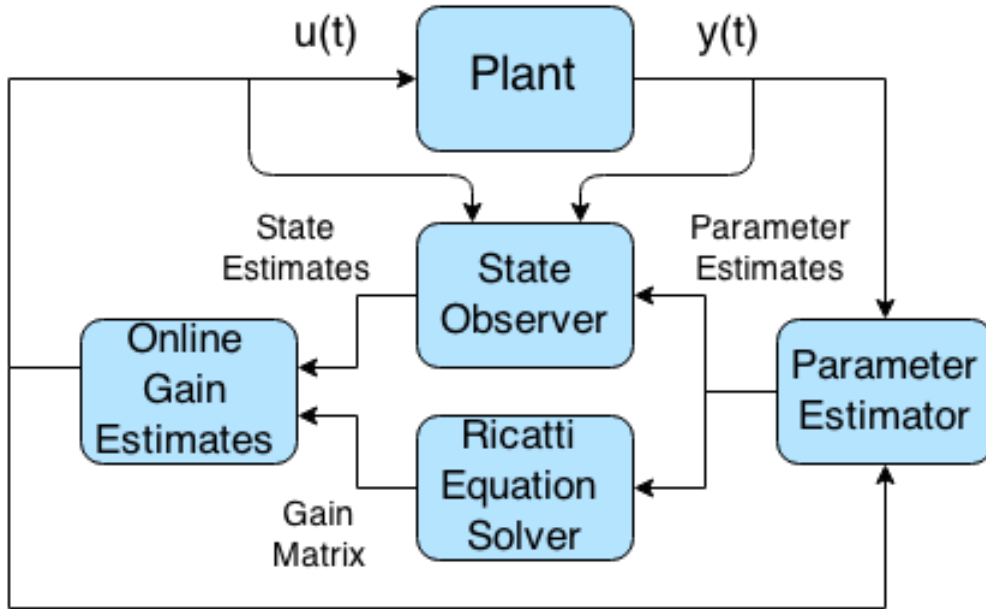


Figure 3.1: Block diagram of the adaptive LQ control system.

system matrix estimate pair  $(\hat{A}_g(t), \hat{B}_g(t))$  is stabilizable and  $(\hat{A}_g(t), C_g)$  is detectable. To guarantee this we must examine the controllability and observability of our system for all time.

Controllability for the matrix pair  $(\hat{A}_g(t), \hat{B}_g(t))$  at the frozen time  $t$  is given by the equation

$$C = [\hat{B}_g \quad \hat{A}_g \hat{B}_g \quad \hat{A}_g^2 \hat{B}_g \quad \hat{A}_g^3 \hat{B}_g \quad \hat{A}_g^4 \hat{B}_g \quad \hat{A}_g^5 \hat{B}_g]. \quad (3.34)$$

While the controllability matrix for the pair  $(A_g, B_g)$  is too large to be practically included here, it was shown previously that this pair is controllable in all scenarios except for the following:

- The system parameter estimate  $\hat{f} \neq 0$ .
- The system parameter estimate  $\hat{g} \neq 0$ .
- The system parameter estimates  $\hat{\eta}, \hat{\zeta}$  are such that  $\hat{\eta} \neq \hat{\zeta} \neq 0$  simultaneously.

These are the same conditions as given in Section 3.2 where each parameter is replaced with its adaptive estimate. For all other values of  $\hat{f}, \hat{g}, \hat{\eta}, \hat{\zeta}$ , it can be shown that the controllability matrix has full rank which gives us controllability of the matrix pair  $(\hat{A}_g, \hat{B}_g)$ . For simplicity we can impose the condition that  $\hat{f} \neq 0, \hat{g} \neq 0, \hat{\eta} \neq 0, \hat{\zeta} \neq 0$ , which is inclusive of the three conditions given above. Then, given assumption (A3), this allows us to apply parameter projection to guarantee that the all parameters never cross zero, ensuring that the pair  $(\hat{A}_g(t), \hat{B}_g(t))$  is controllable for all time (See Section 3.3.2 for details).

Observability for this system model is much simpler to ensure. Since we are in MIMO observer canonical form, the observability matrix, given by

$$\mathcal{O} = \begin{bmatrix} C_g \\ C_g \hat{A}_g \\ C_g \hat{A}_g^2 \\ C_g \hat{A}_g^3 \\ C_g \hat{A}_g^4 \\ C_g \hat{A}_g^5 \end{bmatrix}, \quad (3.35)$$

will always have full rank regardless of the value of the parameters  $\hat{f}, \hat{g}, \hat{\eta}, \hat{\zeta}$ . As such, the matrix pair  $(\hat{A}_g(t), C_g)$  will be observable for all time. This analysis shows that assumptions (A1)–(A3) are sufficient to guarantee that the adaptive Riccati equation in (3.31) has a finite, unique positive definite solution  $P$  for all time.

**Stability analysis.** We will now show that the observer error dynamic equation is stable which can be shown to lead to stability of the overall system. We begin by proposing the following lemma.

**Lemma 3.3.1** *Given assumptions (A1)–(A3), the indirect adaptive control scheme in equations (3.30)–(3.33) guarantees local stability and boundedness of all closed-loop signals.*

*Proof:* Since the control law (3.30) results in the closed-loop observer state equation

$$\begin{aligned}\dot{\hat{x}} &= (\hat{A}_g - \hat{B}_g R^{-1} \hat{B}_g^T P) \hat{x} - \hat{K}_o (C_g \hat{x} - y) \\ &= A_c(t) \hat{x} + \hat{K}_o C_g e_o\end{aligned}\tag{3.36}$$

where  $e_o = x - \hat{x}$  is the observation error, and the observer is chosen to be stable, it follows that we need to establish the stability of  $A_c(t)$ . With assumptions (A1), (A3) and this system structure, the online estimates  $(\hat{A}_g, \hat{B}_g)$  are stabilizable. Then, at each frozen time  $t$ , we can say that all eigenvalues of  $A_c(t)$  have negative real parts. To conclude stability, we then need to show that  $\|\dot{A}_c(t)\| \in L^2$ . For this, we take the norm of  $\dot{A}_c(t)$  to obtain the relationship:

$$\begin{aligned}\|\dot{A}_c(t)\| &\leq \|\dot{\hat{A}}_g(t)\| + \|\dot{\hat{B}}_g(t)\| R^{-1} \|\hat{B}_g^T(t)\| \|P(t)\| \\ &+ \|\hat{B}_g(t)\| R^{-1} \|\dot{\hat{B}}_g^T(t)\| \|P(t)\| + \|\hat{B}_g(t)\| R^{-1} \|\hat{B}_g^T(t)\| \|\dot{P}(t)\|.\end{aligned}\tag{3.37}$$

To obtain an expression for  $\dot{P}$ , take the derivative of (3.31):

$$\begin{aligned}&\frac{d}{dt} (\hat{A}_g^T(t) P(t) + P(t) \hat{A}_g(t) - P(t) \hat{B}_g(t) R^{-1} \hat{B}_g^T(t) P(t) + Q) \\ &= \dot{\hat{A}}_g^T P + \hat{A}_g^T \dot{P} + \dot{P} \hat{A}_g + P \dot{\hat{A}}_g - \dot{P} \hat{B}_g R^{-1} \hat{B}_g^T P \\ &- P \dot{\hat{B}}_g R^{-1} \hat{B}_g^T P - P \hat{B}_g R^{-1} \dot{\hat{B}}_g^T P - P \hat{B}_g R^{-1} \hat{B}_g^T \dot{P} = 0\end{aligned}\tag{3.38}$$

which can be organized as

$$\begin{aligned} & \hat{A}_g^T \dot{P} + \dot{P} \hat{A}_g - \dot{P} \hat{B}_g R^{-1} \hat{B}_g^T P - P \hat{B}_g R^{-1} \hat{B}_g^T \dot{P} \\ & = -\dot{\hat{A}}_g^T P - P \dot{\hat{A}}_g + P \dot{\hat{B}}_g R^{-1} \hat{B}_g^T P + P \hat{B}_g R^{-1} \dot{\hat{B}}_g^T P. \end{aligned} \quad (3.39)$$

Finally, we arrive at

$$A_c^T \dot{P} + \dot{P} A_c = -Q, \quad (3.40)$$

where

$$Q = \dot{\hat{A}}_g^T P + P \dot{\hat{A}}_g - P \dot{\hat{B}}_g R^{-1} \hat{B}_g^T P - P \hat{B}_g R^{-1} \dot{\hat{B}}_g^T P. \quad (3.41)$$

Since at any frozen time  $t$ , all eigenvalues of  $A_c(t)$  have negative real part, then for any given  $\hat{A}_g, \hat{B}_g, P$ , equation (3.40) is a Sylvester Equation of the form

$$AX + XB = C \quad (3.42)$$

where  $A, B, C$  are arbitrary  $n \times n$  matrices. The solution to the Sylvester Equation is guaranteed to exist when  $A$  and  $-B$  have no common eigenvalues. Then, for (3.40), we see that  $A_c(t)$  and  $-A_c(t)$  have no common eigenvalues. Thus, we have that the solution  $\dot{P}$  exists and is continuous with respect to  $Q$ . Given Assumption (A2), this leads to  $P \in L^\infty$  and  $\|\dot{P}(t)\| \in L^2$ . Thus we have  $\dot{A}_c(t) \in L^2$  and we can conclude that  $A_c(t)$  is a uniformly asymptotically stable matrix. It follows from this and assumption (A2) that all closed-loop signals are bounded using the techniques found within [5].

▽

### 3.3.2 Parameter Estimation

In order to implement an indirect adaptive control scheme, we construct an adaptive parameter estimator to estimate the uncertain parameters. For this estimator, we will choose to only estimate the unknown physical plant parameters  $f, g, \eta, \zeta$ . This gives us an advantage over certain direct adaptive control schemes where it may be required to estimate many more uncertain parameters that may be comprised of products and powers of the physical parameters. Due to the symmetry of the problem with the uncertain parameters in (2.40) we will construct an estimator for the uncertain parameters of the first equation only.

#### Parametric Model

We will begin our design by neglecting the effects of noise by letting  $\chi = 0$  in (2.40). Then the dynamic equation for  $y_1$  becomes

$$\ddot{y}_1 + f\ddot{y}_1 + \eta\dot{y}_1 - \zeta\dot{y}_2 + f\eta y_1 + f\zeta y_2 + g\ddot{u}_2 - fg\dot{u}_2 = 0. \quad (3.43)$$

Similar to that used in [1], for adaptive law derivation and implementation purposes, we will construct three third-order filters in order to measure the derivatives of  $y_1, y_2, u_2$ . The first filter system is

$$\begin{aligned} \dot{\phi}_1 &= \phi_2 \\ \dot{\phi}_2 &= \phi_3 \\ \dot{\phi}_3 &= -l_0\phi_1 - l_1\phi_2 - l_2\phi_3 + y_1, \end{aligned} \quad (3.44)$$

the second filter system is

$$\begin{aligned}\dot{\psi}_1 &= \psi_2 \\ \dot{\psi}_2 &= \psi_3 \\ \dot{\psi}_3 &= -l_0\psi_1 - l_1\psi_2 - l_2\psi_3 + y_2,\end{aligned}\tag{3.45}$$

and the third filter system is

$$\begin{aligned}\dot{\omega}_1 &= \omega_2 \\ \dot{\omega}_2 &= \omega_3 \\ \dot{\omega}_3 &= -l_0\omega_1 - l_1\omega_2 - l_2\omega_3 + u_2.\end{aligned}\tag{3.46}$$

Here,  $l(s) = s^3 + l_2s^2 + l_1s + l_0$  is chosen as a monic and stable polynomial. Then, operating  $l(s)$  on  $y_1$  we obtain

$$l(s)[y_1](t) = \ddot{y}_1 + l_2\dot{y}_1 + l_1\dot{y}_1 + l_0y_1.\tag{3.47}$$

Combining this equation with (3.43), we obtain

$$\begin{aligned}l(s)[y_1] &= \ddot{y}_1 + l_2\dot{y}_1 + l_1\dot{y}_1 + l_0y_1 - (\ddot{y}_1 + f\dot{y}_1 \\ &+ \eta\dot{y}_1 - \zeta\dot{y}_2 + f\eta y_1 + f\zeta y_2 + g\ddot{u}_2 - fg\dot{u}_2).\end{aligned}\tag{3.48}$$

Operating both sides by  $\frac{1}{l(s)}$  and using our three filter systems, we obtain

$$\begin{aligned}y_1(t) &= l_2\phi_3 + l_1\phi_2 + l_0\phi_1 - f\phi_3 - \eta\phi_2 + \zeta\psi_2 \\ &- f\eta\phi_1 - f\zeta\psi_1 - g\omega_3 + fg\omega_2.\end{aligned}\tag{3.49}$$

This is our parametric model for the system in (3.12), neglecting the noise term. This equation can be further written as

$$\begin{aligned} y_1 - l_2\phi_3 - l_1\phi_2 - l_0\phi_1 + \eta\phi_2 - \zeta\psi_2 \\ + g\omega_3 + f(\phi_3 + \eta\phi_1 + \zeta\psi_1 - g\omega_2) = 0. \end{aligned} \quad (3.50)$$

### Parameter Update Law

Based on (3.50), with the estimates  $\hat{\eta}, \hat{\zeta}, \hat{g}, \hat{f}$  of  $\eta, \zeta, g, f$ , we define the estimation error

$$\begin{aligned} \epsilon = y_1 - l_2\phi_3 - l_1\phi_2 - l_0\phi_1 + \hat{\eta}\phi_2 - \hat{\zeta}\psi_2 \\ + \hat{g}\omega_3 + \hat{f}(\phi_3 + \hat{\eta}\phi_1 + \hat{\zeta}\psi_1 - \hat{g}\omega_2). \end{aligned} \quad (3.51)$$

From (3.51), as given in [1], it follows that

$$\epsilon = -\Omega^T \tilde{\theta} + \tilde{\theta}^T \Sigma \tilde{\theta}, \quad (3.52)$$

where the parameter error is  $\tilde{\theta} = \theta - \hat{\theta}(t)$ , with  $\theta$  and  $\hat{\theta}(t)$  being the parameter vector and its online estimate vector, given as

$$\theta = \begin{bmatrix} \eta \\ \zeta \\ g \\ f \end{bmatrix}, \quad \hat{\theta}(t) = \begin{bmatrix} \hat{\eta} \\ \hat{\zeta} \\ \hat{g} \\ \hat{f} \end{bmatrix}. \quad (3.53)$$

The regressor vector  $\Omega$  is

$$\Omega = \begin{bmatrix} \phi_2 + \hat{f}\phi_1 \\ -\psi_2 + \hat{f}\psi_1 \\ \omega_3 - \hat{f}\omega_2 \\ \phi_3 + \hat{\eta}\phi_1 + \hat{\zeta}\psi - \hat{g}\omega_2 \end{bmatrix}, \quad (3.54)$$

and the matrix  $\Sigma$  is

$$\Sigma = \begin{bmatrix} 0 & 0 & 0 & 0 \\ 0 & 0 & 0 & 0 \\ 0 & 0 & 0 & 0 \\ -\phi_1 & -\psi_1 & \omega_2 & 0 \end{bmatrix}. \quad (3.55)$$

With the definition of the estimation error  $\epsilon(t)$ , we can design a gradient parameter estimator with the update law [1]:

$$\dot{\hat{\theta}} = -\Gamma \frac{\Omega \epsilon}{1 + \gamma \Omega^T \Omega} + f_p(t) \quad (3.56)$$

where  $\gamma$  is a positive constant and  $\Gamma = \Gamma^T > 0$  is a constant positive definite symmetric matrix. The projection signal  $f_p(t)$  is used to ensure controllability of the pair  $(\hat{A}_g, \hat{B}_g)$  for all time. With assumption (A3), this is accomplished by designing the projection signal as

$$f_{pi}(t) = \begin{cases} 0 & \text{if } |\hat{\theta}_i(t)| \in [0, \infty] \text{ or} \\ & \text{if } \hat{\theta}_i(t) = 0 \text{ and } \text{sign}[\theta_i]g_i(t) \geq 0 \text{ or} \\ -g_i(t) & \text{otherwise} \end{cases} \quad (3.57)$$

This projection operator guarantees that each estimate  $\hat{f}, \hat{g}, \hat{\eta}, \hat{\zeta}$  never crosses zero. This satisfies the controllability requirement and ensures that the Riccati equation (3.31) has a solution. Analysis of this parameter estimator reveals that it is locally

stable [1]. Such an adaptive law ensures that  $\hat{\theta}, \dot{\hat{\theta}}, \frac{\epsilon}{m}$  are bounded and  $\dot{\hat{\theta}}, \frac{\epsilon}{m} \in L_2$  for  $m = \sqrt{1 + \gamma\Omega^T\Omega}$ , locally or globally.

### Parameter Update Law for the Case with Noise

Now we consider the case where the noise  $\chi \neq 0$  in (3.12). The parameter projection technique can be used to provide robustness in the presence of bounded noise, however we address another viable technique here.

Since the input to the system is noisy, there is the potential for parameter drift due to small estimation errors caused by the noise. To counteract such a noise for robustness, we need to modify the adaptive law. We first introduce a deadzone nonlinearity  $\Delta(\cdot; b)$  defined as

$$\Delta(\epsilon; b) = \begin{cases} \epsilon & \text{if } |\epsilon| > b \\ 0 & \text{if } |\epsilon| \leq b \end{cases}$$

for some constant  $b > 0$ . Then, the adaptive parameter update law is modified as

$$\dot{\hat{\theta}} = -\Gamma \frac{\Omega\Delta(\epsilon; b)}{1 + \gamma\Omega^T\Omega}. \quad (3.58)$$

The function of the deadzone nonlinearity  $\Delta(\cdot; b)$  is to stop the parameter adaptation if the estimation error  $\epsilon(t)$  is below a specific value  $b$ . This technique may be combined with parameter projection to guarantee the existence of a solution to the online Riccati equation (3.31) for all time and is a viable technique in many applications for the rejection of input noise and guarantees that our parameter estimates remain bounded.

## 3.4 Simulation Study

In this section we will demonstrate the ability of our adaptive controller to successfully stabilize the system under non-ideal circumstances such as exposure to a noisy input signal, actuator saturation, and a shift in system parameters. We will provide a recap of the system and controller, then discuss the simulation conditions, and finally provide a summary of our simulation results.

### 3.4.1 System Model

Recall that the time delayed jet engine system model was approximated by a non-minimum phase system model

$$A(s)y = B(s)u + C(s)\chi \quad (3.59)$$

where  $A(s), B(s), C(s)$  are given as

$$\begin{aligned} A(s) &= Is^3 + fIs^2 + Q_1^T s + fQ_1 \\ B(s) &= g(f - s)sP_1 \\ C(s) &= h(s + f)I \\ Q_1 &= \eta I + \zeta P_1 \\ P_1 &= \begin{bmatrix} 0 & 1 \\ -1 & 0 \end{bmatrix}. \end{aligned} \quad (3.60)$$

It was built in MATLAB in the state variable form with  $x(t) \in R^6$  and a state observer with  $\hat{x}(t) \in R^6$ :

$$\dot{x} = A_g x + B_g u + D_g \chi, \quad y = C_g x \quad (3.61)$$

$$\dot{\hat{x}} = \hat{A}_g \hat{x} + \hat{B}_g u - \hat{K}_o (C_g \hat{x} - y). \quad (3.62)$$

The uncertain parameters  $\eta, \zeta, f, g$  were estimated according to the adaptive update law

$$\dot{\hat{\theta}} = -\Gamma \frac{\Omega \Delta(\epsilon; b)}{1 + \gamma \Omega^T \Omega} \quad (3.63)$$

where  $\epsilon$  is the estimation error,  $\Omega$  is the regressor vector, and  $\hat{\theta}$  is the estimate of the parameter vector,  $\Delta(\cdot; b)$  is a deadzone nonlinearity to help reject noise errors in the estimator. The adaptive LQ control law was

$$u = -\hat{K} \hat{x} \quad (3.64)$$

which was constructed by creating estimates  $\hat{A}_g(t), \hat{B}_g(t)$  of the system matrices  $A_g, B_g$  and using them to solve the online Riccati Equation

$$\hat{A}_g^T(t)P(t) + P(t)\hat{A}_g(t) - P(t)\hat{B}_g(t)R^{-1}\hat{B}_g^T(t)P(t) + Q = 0 \quad (3.65)$$

for the matrix  $P(t)$  to construct the control gain

$$\hat{K} = R^{-1}\hat{B}_g^T(t)P(t). \quad (3.66)$$

### 3.4.2 Simulation Conditions and Cases

Due to the lack of real world values of the unknown parameters, this system was simulated against the same values as the simulation done in [1]. Additionally, their choice of initial conditions were also used as they are representative of what one would use as an initial estimate of the unknown parameters. These conditions and values are listed below:

- $f = g = \eta = \zeta = h = 1$
- $y_1(0) = 1, y_2(0) = 1$
- $\hat{\eta}(0) = 1.3\eta$ : This parameter is the natural frequency of the closed-loop plant, and is least uncertain.
- $\hat{g}(0) = 2g$ : This parameter is estimated large because we have limited control authority and an underestimate would lead to the need for large input values.
- $\hat{f}(0) = 2.4f$ : This is chosen large so as to not underestimate the system time delay.
- $\hat{\zeta}(0) = 1.7\zeta$ : We overestimate the coupling, as a low estimate would imply a predominantly SISO design.
- $\Gamma = 10I, \gamma = 1$
- $b = 0.03$ : This parameter determines the deadzone size to help to avoid bursting due to noisy inputs.

The rest of the simulation parameters are as follows:

- $R = 10I$ : This was chosen large so as to help limit large transient values in the control input.
- $l(s) = s^3 + 6s^2 + 11s + 6$
- The poles of  $A_o^*(s)$  were chosen to be sufficiently fast.

With these parameter values the open-loop plant is unstable with poles at  $-1.3 \pm j0.75, 0.11 \pm j1.4, 0.23 \pm j0.63$ .

Three different cases were studied for comparison with our adaptive control scheme. These cases are as follows:

- Case I: the ideal controller with no adaptation,  $\hat{\theta} = \theta$ .
- Case II: a non-adaptive controller with  $\hat{\eta} = 1.3\eta, \hat{g} = 2g, \hat{f} = 2.4f, \hat{\zeta} = 1.7\zeta$
- Case III: the adaptive controller with  $\hat{\eta}(0) = 1.3\eta, \hat{g}(0) = 2g, \hat{f}(0) = 2.4f, \hat{\zeta}(0) = 1.7\zeta$ .

We conducted four sets of simulations, each with the three cases as mentioned above, under different circumstances. In the first simulation set we chose the weighting  $Q = I$ , as for LQ control the requirement is that  $Q$  must be positive semidefinite. In our second simulation set we chose  $Q = C_g^T C_g$  as this is a common choice of  $Q$  since it results in the cost function depending only upon the output vector  $y$ . Our third simulation set contained a shift in parameter values to simulate a fundamental change in the system. The last simulation set contained the same parameter shift as well as a limit on the range of the control input in order to simulate the potential for actuator saturation.

### 3.4.3 Simulation Results for $Q = I$

Fig. 3.2–3.3 show the outputs and inputs of the system, respectively, for different controllers. As we can see for the adaptive case, during the adaptation phase from 0 to around 10 seconds, the output grows in magnitude. After this, Fig. 3.4 shows that the parameter estimates have settled and the origin becomes stable. The magnitude of the output then begins to decay and approaches zero around 20 seconds. Fig. 3.5 shows the estimation error  $\epsilon(t)$ . As we can see, it also approaches zero, which is to be expected as that is guaranteed by the adaptive law. The parameter estimates in Fig. 3.4 do not approach the true values because of a lack of persistence of excitation, however, this is unnecessary for achieving the desired control objective, since the estimation error is always guaranteed to go to zero.

Figures 3.2 and 3.3 also show outputs and inputs for the ideal and non-ideal fixed gain controllers as a comparison. As is easily seen, the adaptive controller performs much better than the non-ideal case as this case is unstable and the outputs and inputs diverge due to poor initial estimates.

### 3.4.4 Simulation Results for $Q = C_g^T C_g$

One common choice of  $Q$  is to set it as  $Q = C_g^T C_g$ . This is because such a choice of  $Q$  will lead to the cost function term  $x^T Q x = x^T C_g^T C_g x = y^T y$ . Then, our optimality is based upon the magnitude of the control inputs and system outputs. As we can see in Figs. 3.6 and 3.7 for the adaptive case, during the adaptation phase from 0 to around 10 seconds, the output grows in magnitude. After this, Fig. 3.8 shows that the parameter estimates have settled and the origin becomes stable. The magnitude of the output then begins to decay and approaches zero around 20 seconds. The parameter estimates in Fig. 3.8 do not approach the true values because of a lack

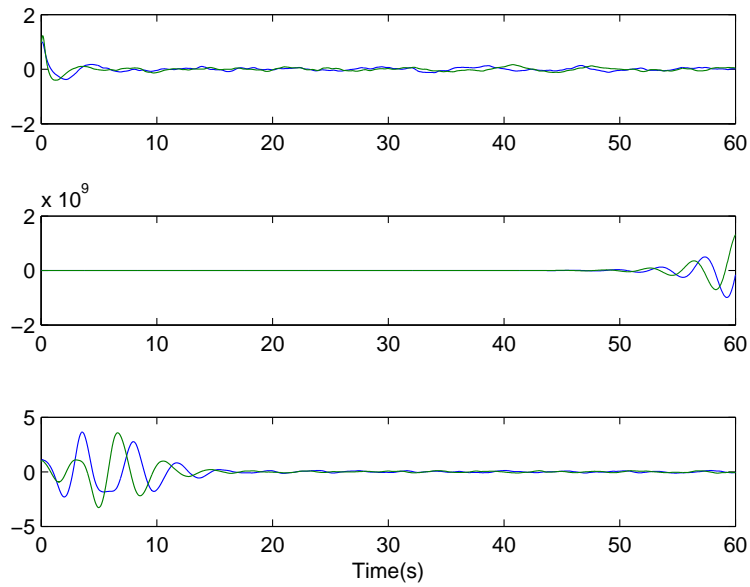


Figure 3.2: System outputs for  $Q = I$  case with ideal controller (top), non-ideal controller (middle) and adaptive controller (bottom).

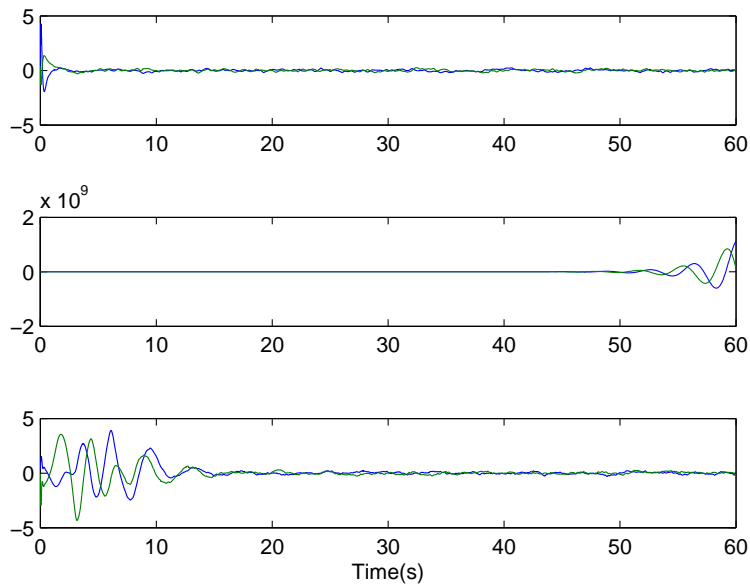


Figure 3.3: Control inputs for  $Q = I$  case with ideal controller (top), non-ideal controller (middle), and adaptive controller (bottom).

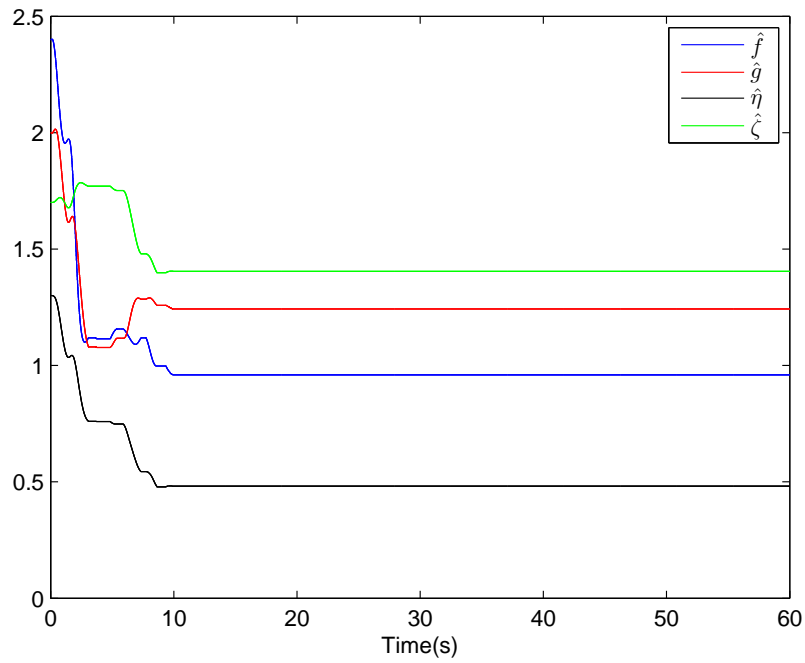


Figure 3.4: Adaptive parameter estimates  $\hat{\eta}, \hat{\zeta}, \hat{g}, \hat{f}$  for  $Q = I$  case.

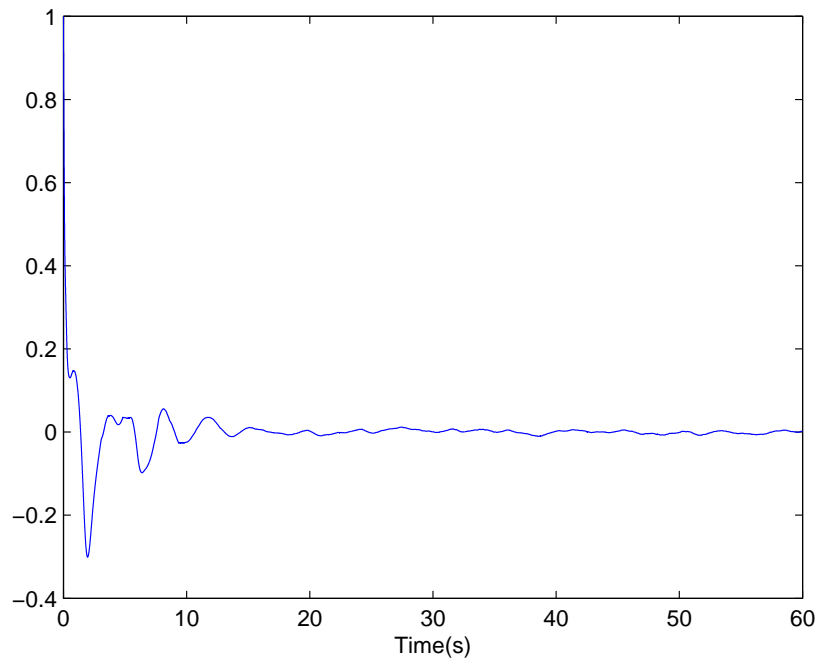


Figure 3.5: Output estimation error  $\epsilon(t)$  for  $Q = I$  case.

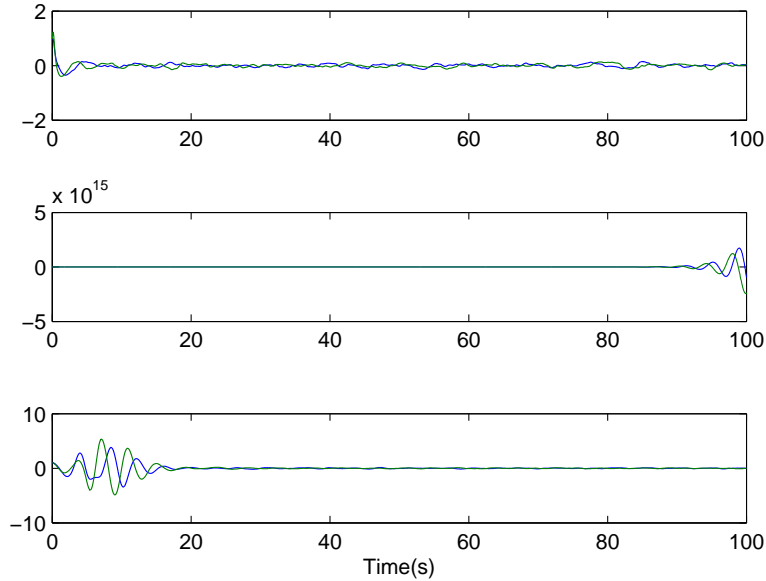


Figure 3.6: System outputs for  $Q = C_g^T C_g$  case with ideal controller (top), non-ideal controller (middle) and adaptive controller (bottom).

of the persistence of excitation condition, however, this is unnecessary for achieving the desired control objective, since the estimation error is always guaranteed to go to zero.

Fig. 3.6 and 3.7 also show outputs and inputs for the ideal and non-ideal fixed gain controllers as a comparison. As is easily seen, the adaptive controller performs much better than the non-ideal case as this case is unstable and the outputs and inputs diverge due to poor initial estimates.

### 3.4.5 Simulation Results for Parameter Jump Case

This case is one that has received a lot of attention from the research community in recent years. Parameter jump can result from a number of physical phenomena, all of which represent the system undergoing sudden change due to the occurrence

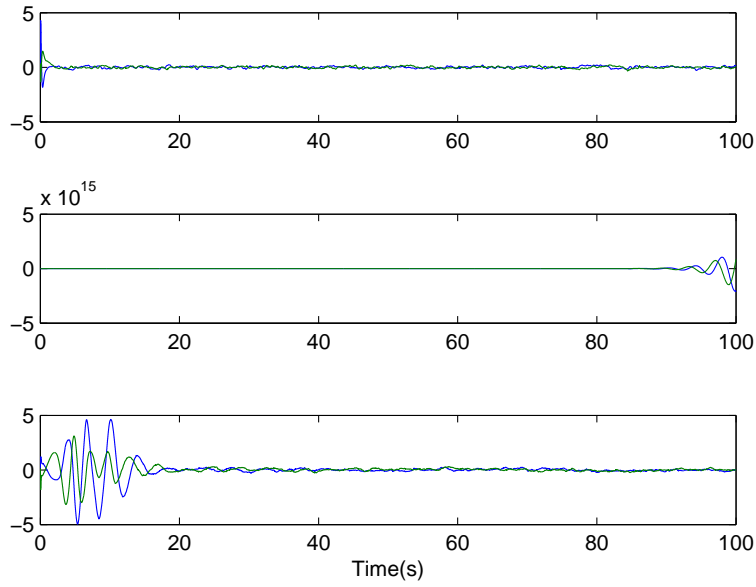


Figure 3.7: Control inputs for  $Q = C_g^T C_g$  case with ideal controller (top), non-ideal controller (middle) and adaptive controller (bottom).

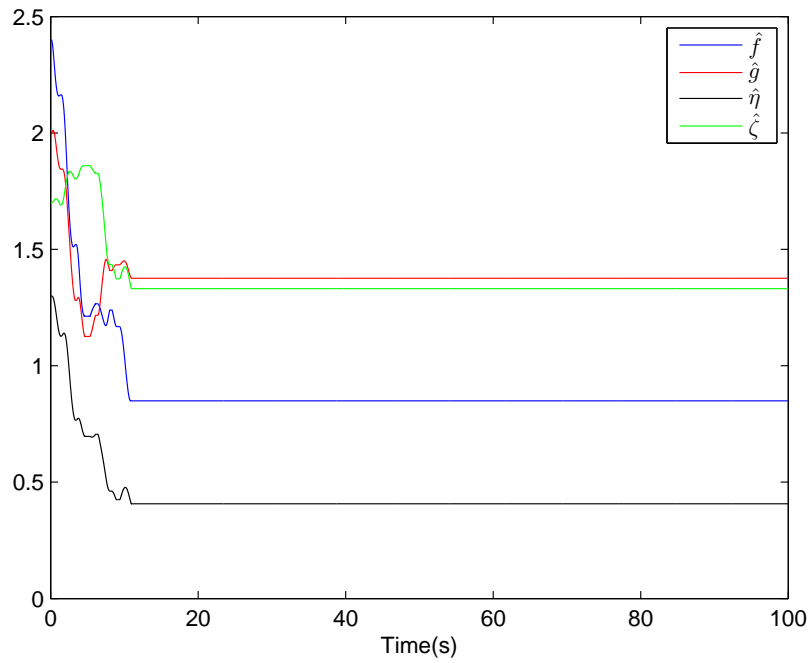


Figure 3.8: Adaptive parameter estimates  $\hat{\eta}, \hat{\zeta}, \hat{g}, \hat{f}$  for  $Q = C_g^T C_g$  case.

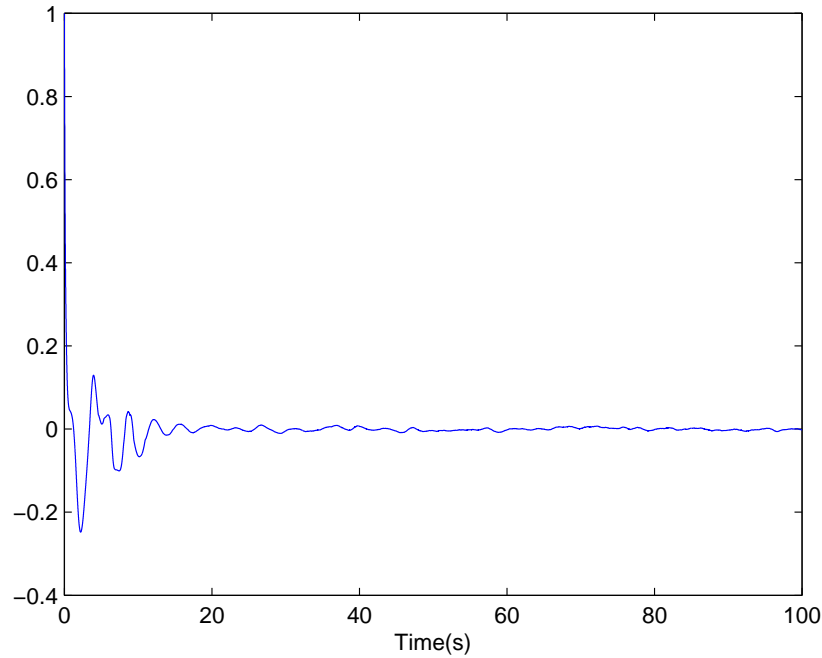


Figure 3.9: Output estimation error  $\epsilon(t)$  for  $Q = C_g^T C_g$  case.

of events such as structural damage. In this simulation we chose a parameter jump for the unknown physical parameters  $f, g, \eta, \zeta$ . Due to lack of real world values for these parameters we will choose all parameters to jump to a value of 1.5 starting at  $t = 30$  and moving linearly to their final values over a 50 second period. Outputs and control inputs can be seen in Fig. 3.10–3.11. At the initial time of the parameter jump, as can be seen in Fig. 3.12–3.13 the parameter values do not change due to the estimation error lying within the deadzone; however when the error grows, the parameter estimator updates and the controller is able to compensate. A second peak occurs after the parameter jump for a similar reason as the first peak occurred - the estimation error was within the deadzone while the parameter jump was occurring. Fig. 3.12 shows that after around 80 seconds the estimator has stopped adapting, and the origin becomes stable again.

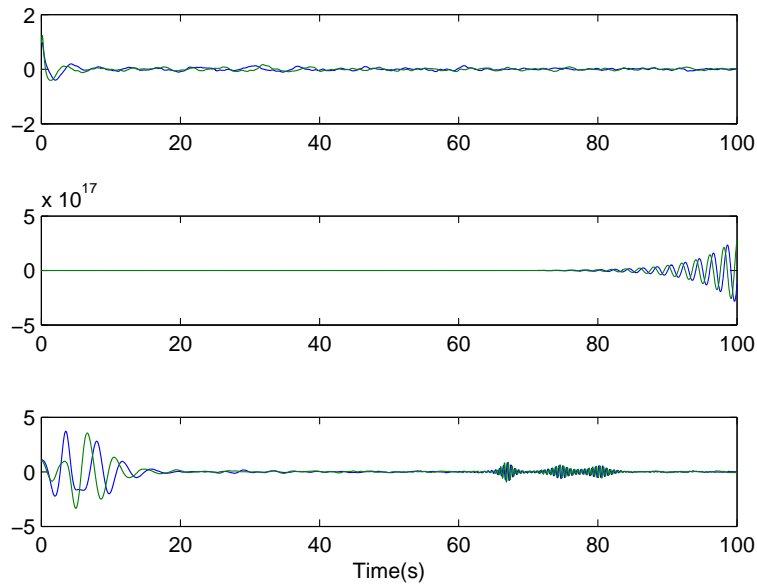


Figure 3.10: System outputs for the parameter jump case with ideal controller (top), non-ideal controller (middle) and adaptive controller (bottom).

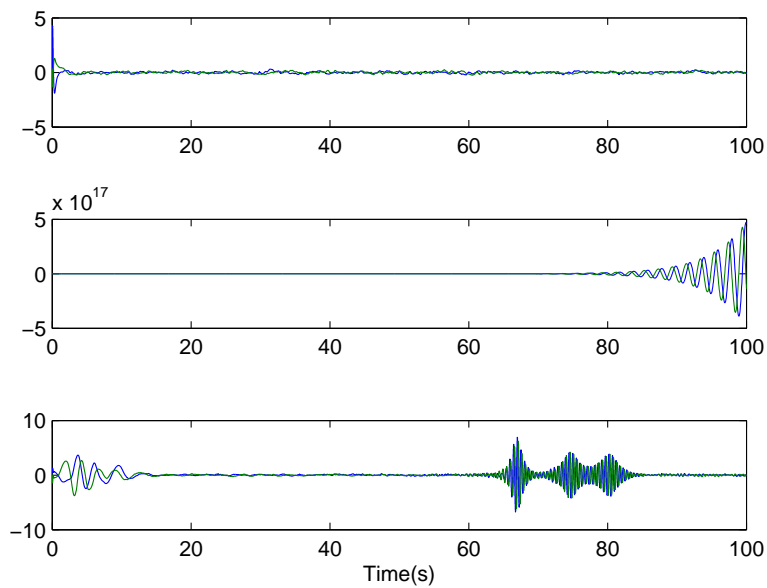


Figure 3.11: Control inputs for the parameter jump case with ideal controller (top), non-ideal controller (middle) and adaptive controller (bottom).

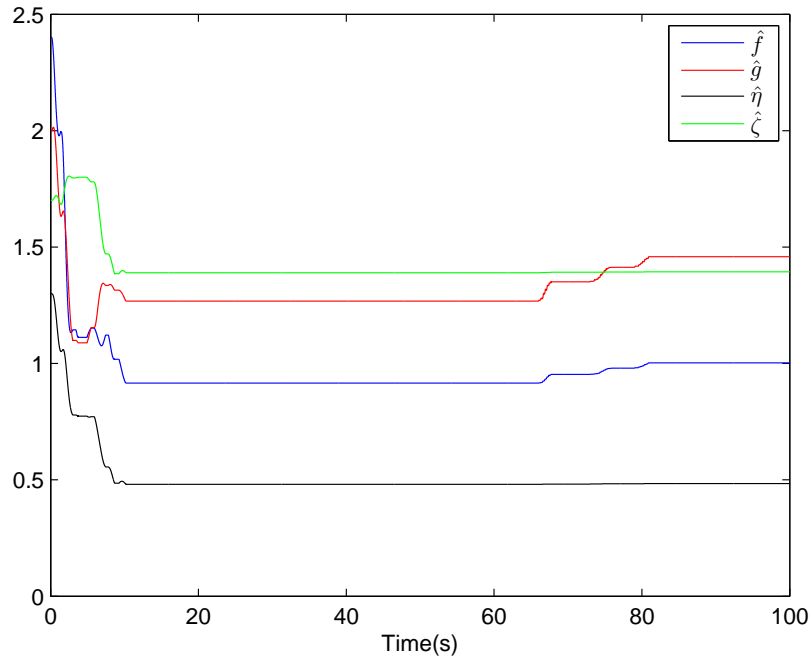


Figure 3.12: Adaptive parameter estimates  $\hat{\eta}$ ,  $\hat{\zeta}$ ,  $\hat{g}$ ,  $\hat{f}$  for the parameter jump case.

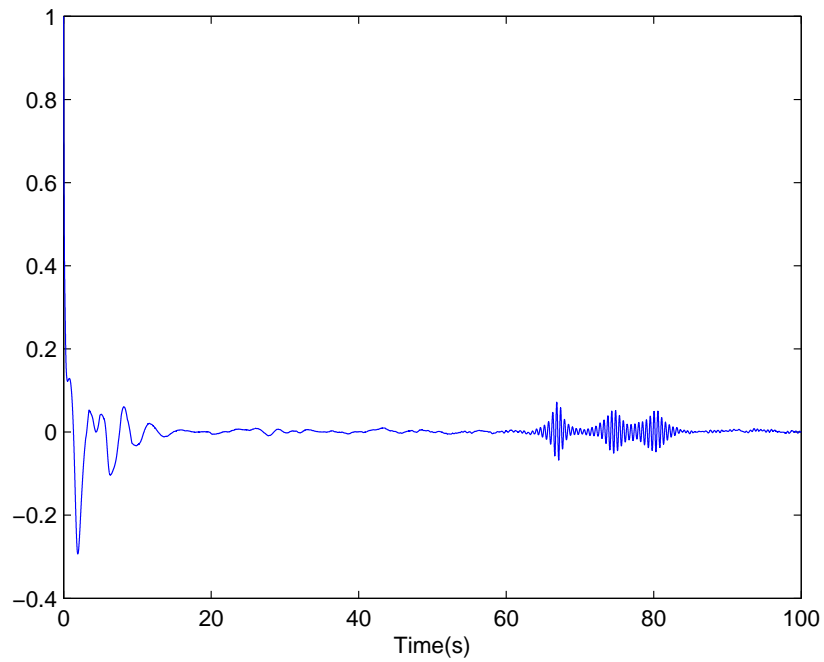


Figure 3.13: Estimation error  $\epsilon(t)$  for the parameter jump case.

### 3.4.6 Simulation Results with Actuator Saturation

An important case to consider in physical systems is actuator saturation. As stated in [1], it is important to note that in this application we have limited control authority, and so we choose to explore the effects of saturation on our control system performance. In this simulation we chose a parameter jump for the unknown physical parameters  $f, g, \eta, \zeta$ . Additionally, we simulate a parameter jump case. Due to lack of real world values for these parameters we will choose all parameters to jump to a value of 1.5 starting at  $t = 30$ , moving linearly to their final values over a 50 second period.

In these simulations, we choose the range of our control input to be  $[-3.5, 3.5]$ . As can be seen in Fig. 3.15, very mild actuator saturation does occur in the initial adaptation phase and Fig. 3.14–3.17 show that the controller does recover from it quite easily. After the parameter jump occurs, the actuators become heavily saturated and work hard to keep the system stabilized, eventually bringing the trajectory back to the origin.

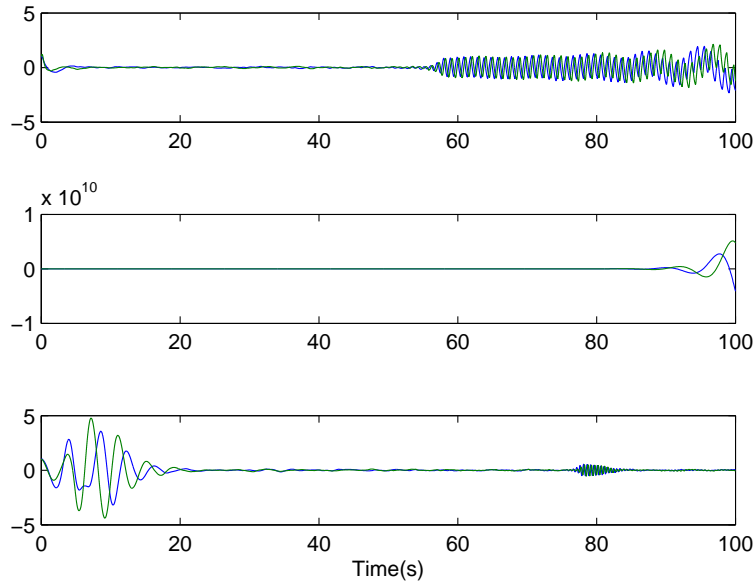


Figure 3.14: System outputs for the parameter jump case with actuator saturation with ideal controller (top), non-ideal controller (middle) and adaptive controller (bottom).

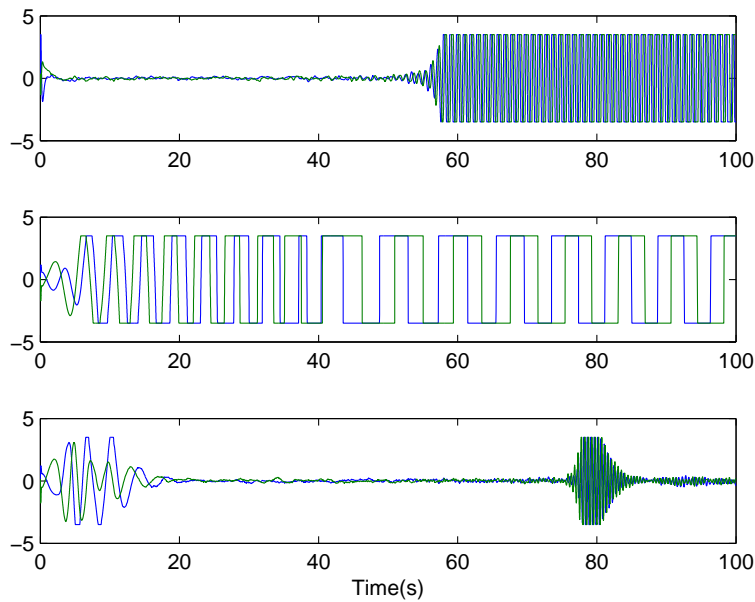


Figure 3.15: Control inputs for the parameter jump case with actuator saturation with ideal controller (top), non-ideal controller (middle) and adaptive controller (bottom).

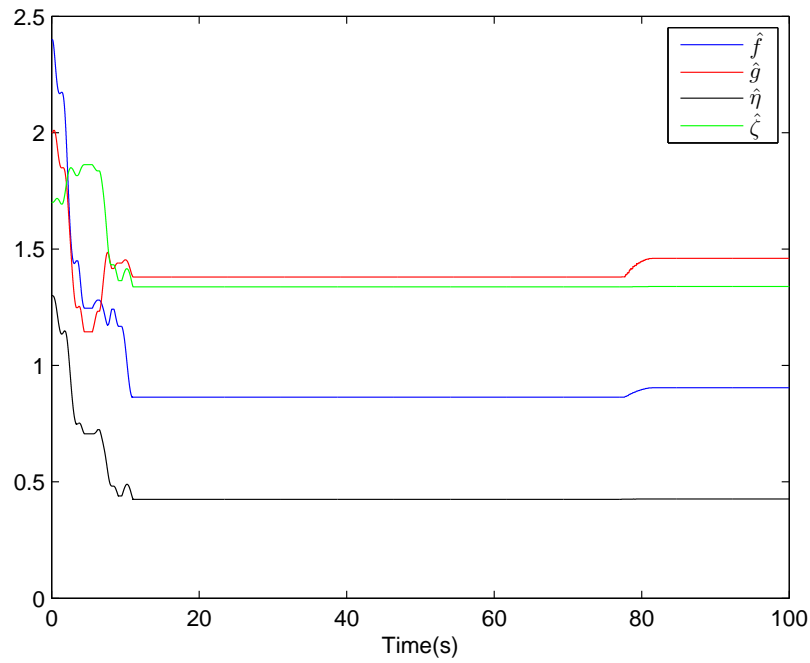


Figure 3.16: Adaptive parameter estimates  $\hat{\eta}$ ,  $\hat{\zeta}$ ,  $\hat{g}$ ,  $\hat{f}$  for the actuator saturation case.

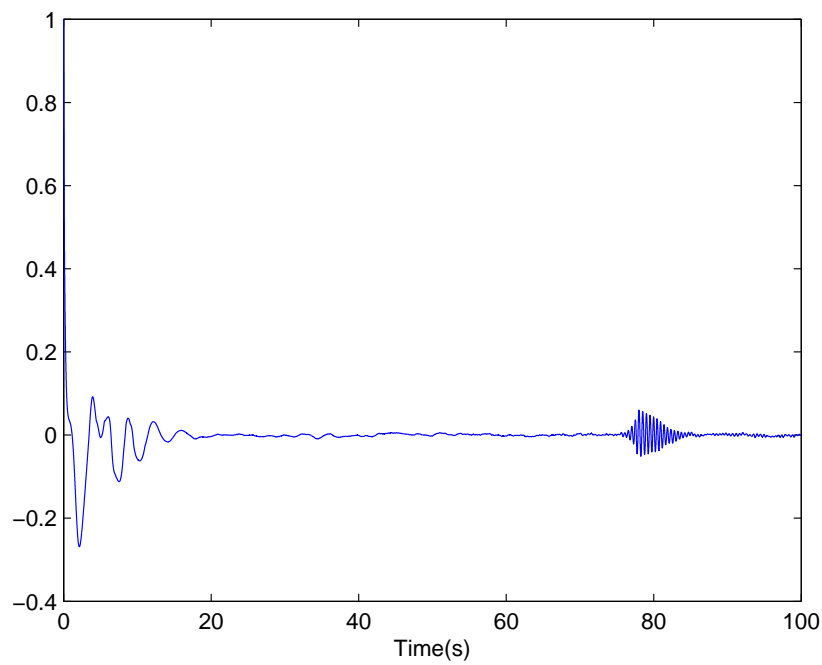


Figure 3.17: Estimation error  $\epsilon(t)$  for the with actuator saturation case.

# Chapter 4

## Backstepping Based Actuator Delay Compensation

When time delays become large, it is no longer appropriate to utilize the Pade approximation since this introduces large modeling errors. Controllers that are designed under the assumption that these modeling errors are sufficiently small when they are not will not be able to guarantee stabilization. Since delays are inherent in the thermoacoustic coupling model given in 2.40, for completeness we are motivated to solve the control problem when time delays may be arbitrarily large. Control of time delay systems has been studied in-depth by the research community. Recent efforts in [17] have led to the development of a backstepping technique that is compatible with adaptive control of systems with unknown arbitrary actuator delay as shown in [19],[20]. This chapter will propose the use an actuator delay compensation scheme by developing a new backstepping transformation that may be used with the simplified thermoacoustic model in 2.40 as well as other systems with both state and actuator delays.

## 4.1 Delay Model

The Pade approximation of a time delayed system is useful for many cases and results in a model that is sufficient for control design; however, there may be difficulties with this method when the time delays are sufficiently long. This means that the modeling error introduced by the approximation is not small enough to ensure that a given controller design will stabilize the system it was designed for. In these circumstances, the system must be modeled with the time delays included in the dynamic equations and the controller designed accordingly.

Similarly to the previous chapter, the equations in (2.40) can be represented as

$$\begin{aligned}(s^2 + \eta)[y_1](t) + \zeta y_2(t - \tau) &= gs[u_2](t - \tau) + h\chi_1 \\ (s^2 + \eta)[y_2](t) - \zeta y_1(t - \tau) &= -gs[u_1](t - \tau) + h\chi_2.\end{aligned}\tag{4.1}$$

These equations can be combined in matrix form as

$$(Is^2 + \eta I)[y](t) + \zeta P_1 y(t - \tau) = gP_1 s[u](t - \tau).\tag{4.2}$$

Using the same approach as in Section 3.1, we find that the state equations for this model with time delays is given as

$$\begin{aligned}\dot{x} &= A_d x + A_{d1} x(t - \tau) + B_d u(t - \tau) + D_d \chi \\ y &= C_d x\end{aligned}\tag{4.3}$$

where

$$A_d = \begin{bmatrix} 0 & I \\ \eta I & 0 \end{bmatrix}, A_{d1} = \begin{bmatrix} 0 & 0 \\ \zeta P_1 & 0 \end{bmatrix}, B_d = \begin{bmatrix} gP_1 \\ 0 \end{bmatrix}, D_d = \begin{bmatrix} 0 \\ hI \end{bmatrix}\tag{4.4}$$

and the output matrix  $C_d$  is known, and is given as

$$C_d = \begin{bmatrix} I & 0 \end{bmatrix}. \quad (4.5)$$

This model can be used with time delay control techniques to solve the standard, non-adaptive control problem. In order to build the theory, the physical parameters  $\eta, \zeta, g, h, \tau$  are assumed to be known. The remainder of this thesis will focus on solving the nominal control problem for the purpose of establishing the foundation for future adaptive control research.

### Input Delay Modeling

The actuator delay compensation scheme that we will develop is based on a method of modeling the input delay term as a transport PDE and will be shown next. Consider the system with arbitrary, potentially long delay given by (4.3). We will begin by neglecting the effects of noise and designing for the system

$$\begin{aligned} \dot{x} &= A_d x(t) + A_{d1} x(t - \tau) + B_d u(t - \tau) \\ y &= C_d x(t) \end{aligned} \quad (4.6)$$

where system matrices  $A_d, A_{d1}, B_d,$  and  $C_d$  are defined as in (4.4) - (4.5). The references in [17] - [21] develop a backstepping transformation for the case where no state delay term exists, that is  $A_{d1} = 0$ . This section will modify that design to be compatible with the case when  $A_{d1} \neq 0$ .

We begin our design by proposing that the delayed input  $u(t - \tau)$  can be expressed

as the boundary response  $v(0, t)$  of the linear transport PDE

$$v_t(s, t) = v_s(s, t) \quad (4.7)$$

under the boundary condition

$$v(\tau, t) = u(t). \quad (4.8)$$

To verify this, we see that  $v(s, t) = u(s + t - \tau)$  satisfies (4.7): for  $g(s, t) = s + t$  we have

$$\begin{aligned} v_s &= u_g(g - \tau)g_s \\ v_t &= u_g(g - \tau)g_t. \end{aligned} \quad (4.9)$$

Since  $g_s = g_t = 1$ , it follows that  $v_s = v_t$ . We also see that  $v(s, t) = u(s + t - \tau)$  satisfies the boundary condition  $v(\tau, t) = u(t)$ . Then, for the solution

$$v(s, t) = u(s + t - \tau) \quad (4.10)$$

at  $s = 0$ , we have  $v(0, t) = u(t - \tau)$ , as expected. Here  $s \in [0, \tau]$  can be viewed as a fictitious distance that the signal  $u(t)$  must propagate in order to act on the system. Because of this, we can choose to model the delayed input term as this transport PDE system without fundamentally changing the system in (4.6). Hence, we can substitute this new model of delay into equation (4.6) to obtain

$$\dot{x} = A_d x(t) + A_{d1} x(t - \tau) + B_d v(0, t) \quad (4.11)$$

$$\begin{aligned} v_t &= v_s \\ v(\tau, t) &= u(t). \end{aligned} \quad (4.12)$$

Writing the system in terms of a transport PDE instead of a delayed input allows us to manipulate the system in beneficial ways, as will be shown next. The goal will be to transform the system into one with desirable properties by way of a backstepping transformation. This transformation will result in obtaining an expression for the control law that is required to achieve a desirable target system.

## 4.2 Backstepping Transformation Design

Our goal for this section is to transform the system (4.11) to one with many desirable properties. Such a desirable system is described as follows:

$$\dot{x} = (A_d + B_d K)x(t) + (A_{d1} + B_d K_1)x(t - \tau) + B_d w(0, t) \quad (4.13)$$

$$w_t = w_s \quad (4.14)$$

$$w(\tau, t) = 0$$

where  $K \in R^{m \times n}$  and  $K_1 \in R^{m \times n}$  are gain matrices that are chosen to stabilize the system, and  $w(s, t)$  is a transform variable. Such gain matrices can be found under the following assumptions:

- (B1) The system matrices  $(A_d, B_d)$  are controllable.
- (B2) Gain matrices  $K$  and  $K_1$  can be found as solutions to the linear matrix inequality

$$\begin{bmatrix} P(A_d + B_d K) + (A_d + B_d K)^T P + \alpha P & P(A_{d1} + B_d K_1) \\ (A_{d1} + B_d K_1)^T P & -\alpha P \end{bmatrix} < 0. \quad (4.15)$$

The LMI in (B2) satisfies the delay-independent stability criteria of the Razumikhin Theorem (see Section 4.3).

To transform to the desired target system given in (4.13)–(4.14), we propose a modified backstepping transformation, defined as

$$\begin{aligned} w(s, t) = v(s, t) - \int_0^s q(s, y)v(y, t)dy - \int_0^s p(s, y)v(y, t - \tau)dy \\ - \gamma(s)^T x(t) - \gamma_1(s)^T x(t - \tau) - f(s, t). \end{aligned} \quad (4.16)$$

Equations (4.14) and (4.16) will result in the control law taking the form

$$\begin{aligned} u(t) = v(\tau, t) = \int_0^\tau q(\tau, y)v(y, t)dy + \int_0^\tau p(\tau, y)v(y, t - \tau)dy \\ + \gamma(\tau)^T x(t) + \gamma_1(\tau)^T x(t - \tau) + f(\tau, t). \end{aligned} \quad (4.17)$$

With the control law (4.17) and the transformation in (4.16), we propose the following lemma:

**Lemma 4.2.1** *Given the Assumptions (B1) and (B2), the modified backstepping transformation given in (4.16) can successfully transform the system in (4.6) to the desired target system in (4.13)–(4.14). Furthermore, given a  $K$  and  $K_1$  chosen to satisfy Assumption (B2), then the backstepping transformation can guarantee exponential stability in terms of the full state norm  $(\|x(t)\|^2 + \int_0^\tau v^2(s, t)ds)^{1/2}$ .*

The remainder of this section will develop the backstepping algorithm needed to obtain the control input that will successfully complete this transformation. We will impose conditions on the functions  $q(s, y)$ ,  $p(s, y)$ ,  $\gamma(s)$ ,  $\gamma_1(s)$ ,  $f(s, t)$  and the control input  $v(\tau, t) = u(t)$  such that we can transform (4.11)–(4.12) to the target system (4.13)–(4.14).

### Backstepping Algorithm

To proceed, we take the partial derivatives of equation (4.16). The derivative  $w_s$  can be obtained by using the Leibniz rule which results in

$$\begin{aligned}
w_s &= v_s - q(s, s)v(s, t) - \int_0^s q_s(s, y)v(y, t)dy \\
&\quad - p(s, s)v(s, t - \tau) - \int_0^s p_s(s, y)v(y, t - \tau)dy \\
&\quad - \gamma'(s)^T x(t) - \gamma'_1(s)^T x(t - \tau) - f_s(s, t)
\end{aligned} \tag{4.18}$$

The derivative  $w_t$  of (4.16) is found by using integration by parts, the fact that  $v_t = v_s$ , and the expression (4.11), that is,

$$\begin{aligned}
w_t &= v_s - q(s, s)v(s, t) + q(s, 0)v(0, t) + \int_0^s q_y(s, y)v(y, t)dy \\
&\quad - p(s, s)v(s, t - \tau) + p(s, 0)v(0, t - \tau) + \int_0^s p_y(s, y)v(y, t - \tau)dy \\
&\quad - \gamma(s)^T [A_d x(t) + A_{d1}x(t - \tau) + B_d v(0, t)] \\
&\quad - \gamma_1(x)^T [A_d x(t - \tau) + A_{d1}x(t - 2\tau) + B_d v(0, t - \tau)] - f_t(s, t).
\end{aligned} \tag{4.19}$$

Since the target system (4.13)–(4.14) requires that  $w_t = w_s$ , subtracting (4.18) from (4.19), we obtain the expression

$$\begin{aligned}
w_t - w_s &= \int_0^s (q_s(s, y) + q_y(s, y))v(y, t)dy + \int_0^s (p_s(s, y) + p_y(s, y))v(y, t - \tau)dy \\
&\quad + [q(s, 0) - \gamma(s)^T B_d]v(0, t) + [p(s, 0) - \gamma_1(s)^T B_d]v(0, t - \tau) \\
&\quad + [\gamma'(s)^T - \gamma(s)^T A_d]x(t) + [\gamma'_1(s)^T - \gamma(s)^T A_{d1} - \gamma_1(s)^T A_d]x(t - \tau) \\
&\quad - \gamma_1(s)^T A_{d1}x(t - 2\tau) - f_t + f_s = 0.
\end{aligned} \tag{4.20}$$

Because we have defined the target system in this way, we can compile a list of conditions that are sufficient to obtain (4.20) as:

$$\begin{aligned} q_s(s, y) + q_y(s, y) &= 0, \\ q(s, 0) &= \gamma(s)^T B_d, \end{aligned} \tag{4.21}$$

$$\begin{aligned} p_s(s, y) + p_y(s, y) &= 0, \\ p(s, 0) &= \gamma_1(s)^T B_d, \end{aligned} \tag{4.22}$$

$$f_s - f_t = g(s, t), \tag{4.23}$$

$$\gamma'(s) = A_d^T \gamma(s), \tag{4.24}$$

$$\gamma_1'(s) = A_d^T \gamma_1(s) + A_{d1}^T \gamma(s), \tag{4.25}$$

where  $g(s, t) = \gamma_1(s)^T A_{d1} x(t - 2\tau)$ . Equations (4.21) and (4.22) represent first-order transport PDEs with their boundary conditions, (4.23) is a nonhomogeneous first-order transport PDE, and the equations (4.24) and (4.25) are first-order ODEs whose initial conditions are obtained from equations (4.11) and (4.16) as well as the boundary condition for (4.23) as shown next. From (4.16), The signal  $v(0, t)$  evaluated from the backstepping equation is given as  $v(0, t) = w(0, t) + \gamma(0)^T x(t) + \gamma_1(0)^T x(t - \tau) + f(0, t)$ . Substituting this into (4.11), we get

$$\begin{aligned} \dot{x} &= A_d x(t) + A_{d1} x(t - \tau) + B_d v(0, t) \\ &= A_d x(t) + A_{d1} x(t - \tau) + B_d (\gamma(0)^T x(t) + \gamma_1(0)^T x(t - \tau) + w(0, t) + f(0, t)) \\ &= (A_d + B_d \gamma(0)^T) x(t) + (A_{d1} + B_d \gamma_1(0)^T) x(t - \tau) + B_d w(0, t) + B_d f(0, t) \end{aligned} \tag{4.26}$$

Comparing this equation with (4.13), we obtain the initial conditions to (4.24), (4.25), and (4.23) as

$$\gamma(0)^T = K. \quad (4.27)$$

$$\gamma_1(0)^T = K_1 \quad (4.28)$$

$$f(0, t) = 0, \quad (4.29)$$

respectively. From this, we can obtain the solution  $\gamma(s)$  to (4.24) as

$$\gamma(s)^T = K e^{A_d s}. \quad (4.30)$$

The solution  $q(s, y)$  of the transport PDE (4.21) can be shown to satisfy

$$\begin{aligned} q(s, y) &= \phi(s - y) \\ q(s, 0) &= \phi(s) \end{aligned} \quad (4.31)$$

where  $\phi(s)$  is the boundary condition of the transport PDE. This can be verified using the boundary condition given in (4.21): we can have the solution  $q(x, y)$  as

$$\begin{aligned} q(s, y) &= \gamma(s - y)^T B_d \\ &= K e^{A_d(s-y)} B_d. \end{aligned} \quad (4.32)$$

Similarly, it can be shown that the solution  $\gamma_1(s)$  to the system (4.25) with initial condition (4.28) is given as

$$\begin{aligned} \gamma_1(s) &= e^{A_d^T(s-s_0)} \gamma_{10} + \int_{s_0}^s e^{A_d^T(s-\sigma)} A_1^T e^{A_d^T \sigma} K^T d\sigma \\ &= e^{A_d^T s} K_1^T + \int_0^s e^{A_d^T(s-\sigma)} A_{d1}^T e^{A_d^T \sigma} K^T d\sigma. \end{aligned} \quad (4.33)$$

It is shown in [22], [23] that a general integral of the form

$$B_{12}(t) = \int_0^t e^{A_{11}(t-s)} A_{12} e^{A_{22}s} ds \quad (4.34)$$

can be evaluated by calculating the matrix exponential

$$e^{\Phi t} = \begin{bmatrix} B_{11}(t) & B_{12}(t) \\ 0 & B_{22}(t) \end{bmatrix} \quad (4.35)$$

and

$$B_{12}(t) = (e^{\Phi t})_{12} \quad (4.36)$$

where  $(\cdot)_{ij}$  denotes the submatrix in row  $i$ , column  $j$  of the given matrix. The matrix  $\Phi$  is an upper-triangular matrix of the form

$$\Phi = \begin{bmatrix} A_{11} & A_{12} \\ 0 & A_{22} \end{bmatrix}. \quad (4.37)$$

This formulation allows us to simplify (4.33). Let

$$\Phi_0 = \begin{bmatrix} A_d^T & A_{d1}^T \\ 0 & A_d^T \end{bmatrix}. \quad (4.38)$$

Then, equation (4.33) simplifies to

$$\gamma_1(s)^T = K_1 e^{A_d s} + K (e^{\Phi_0 s})_{12}^T \quad (4.39)$$

which in turn yields the solution  $p(s, y)$  to the transport PDE system (4.22) as

$$p(s, y) = K_1 e^{A_d(s-y)} + K(e^{\Phi_0(s-y)})_{12}^T. \quad (4.40)$$

Lastly, we shall solve the inhomogeneous hyperbolic PDE system (4.23). This inhomogeneous problem is well understood. To find the solution to this problem, begin by setting  $v(s) = f(s + \sigma, t - \sigma)$ . Then

$$\frac{dv(\sigma)}{d\sigma} = -f_t + f_s(s + \sigma, t - \sigma) = g(s + \sigma, t - \sigma) \quad (4.41)$$

Consider

$$\begin{aligned} f(s, t) - f(0, t + s) &= v(0) - v(-s) \\ &= \int_{-s}^0 \frac{dv}{d\sigma} d\sigma \\ &= \int_{-s}^0 g(s + \sigma, t - \sigma) d\sigma \\ &= \int_0^s g(\sigma, t - (\sigma - s)) d\sigma \end{aligned} \quad (4.42)$$

Given this, we have obtained the solution to the first-order, inhomogeneous transport problem as

$$\begin{aligned} f(s, t) &= f(0, t + s) + \int_0^s g(\sigma, t - (\sigma - s)) d\sigma \\ &= \int_0^s \left[ K_1 e^{A_d\sigma} + K(e^{\Phi_0\sigma})_{12}^T \right] A_{d1} x(t - (\sigma - s) - 2\tau) d\sigma. \end{aligned} \quad (4.43)$$

### Control Law Derivation

Using the solutions obtained in (4.30), (4.32), (4.39), (4.40), (4.43), this process produces the final version of the backstepping transformation

$$\begin{aligned}
w(s, t) = & v(s, t) - \int_0^s K e^{A_d(s-y)} B_d v(y, t) dy \\
& - \int_0^s \left[ \left( K_1 e^{A_d(s-y)} + K (e^{\Phi_0(s-y)})_{12}^T \right) B_d v(y, t - \tau) \right] dy \\
& - \int_0^s \left[ \left( K_1 e^{A_d \sigma} + K (e^{\Phi_0 \sigma})_{12}^T \right) A_{d1} x(t - (\sigma - s) - 2\tau) \right] d\sigma \\
& - K e^{As} x(t) - \left( K_1 e^{As} + K (e^{\Phi_0 s})_{12}^T \right) x(t - \tau)
\end{aligned} \tag{4.44}$$

With all conditions of the transformation equation (4.16) verified, we have that  $v(0, t)$  in equation (4.11) is obtained from (4.16) as

$$v(0, t) = w(0, t) + Kx(t) + K_1 x(t - \tau) \tag{4.45}$$

which results in the desired system (4.13):

$$\dot{x} = (A_d + B_d K)x(t) + (A_{d1} + B_d K_1)x(t - \tau) + B_d w(0, t). \tag{4.46}$$

Lastly, we will complete the transformation and determine the control law by satisfying the  $w(s, t)$  subsystem in (4.14). Because conditions (4.21)-(4.25) have been satisfied, we have that  $w_t = w_s$ . To satisfy the condition  $w(\tau, t) = 0$ , we choose the

control input  $u(t) = v(\tau, t)$  from (4.44) to be

$$\begin{aligned}
v(\tau, t) &= \int_0^\tau K e^{A_d(\tau-y)} B_d v(y, t) dy \\
&+ \int_0^\tau \left[ \left( K_1 e^{A_d(\tau-y)} + K (e^{\Phi_0(\tau-y)})_{12}^T \right) B_d v(y, t - \tau) \right] dy \\
&+ \int_0^\tau \left[ \left( K_1 e^{A_d\sigma} + K (e^{\Phi_0\sigma})_{12}^T \right) A_{d1} x(t - (\sigma - \tau) - 2\tau) \right] d\sigma \\
&+ K e^{A\tau} x(t) + \left( K_1 e^{A\tau} + K (e^{\Phi_0\tau})_{12}^T \right) x(t - \tau).
\end{aligned} \tag{4.47}$$

With this, we have satisfied all conditions of the target system (4.13)–(4.14). The next step is to obtain an expression for the control law  $u(t)$ . Substituting in  $u(t)$  for  $v(\tau, t)$  and using a change of variables, this can be written as

$$\begin{aligned}
u(t) &= \int_{t-\tau}^t K e^{A_d(t-\theta)} B_d u(\theta) d\theta \\
&+ \int_{t-2\tau}^{t-\tau} \left[ \left( K_1 e^{A_d(t-\tau-\theta)} + K (e^{\Phi_0(t-\tau-\theta)})_{12}^T \right) B_d u(\theta) \right] d\theta \\
&+ \int_{t-2\tau}^{t-\tau} \left[ \left( K_1 e^{A_d(t-\tau-\theta)} + K (e^{\Phi_0(t-\tau-\theta)})_{12}^T \right) A_{d1} x(\theta) \right] d\theta \\
&+ K e^{A_d\tau} x(t) + \left( K_1 e^{A_d\tau} + K (e^{\Phi_0\tau})_{12} \right) x(t - \tau).
\end{aligned} \tag{4.48}$$

This control law satisfies all conditions of the backstepping transformation given in (4.16) needed to transform the given system in (4.11) to a desired target system in (4.13)–(4.14). The next section will discuss stability of the delay model when using this controller.

### 4.3 Stability Analysis

As we have satisfied all conditions necessary to transform to the target system (4.13)–(4.14), our analysis will be performed using this as our system model. We will discuss

the delay-independent stability criteria of this system as given by the Razumikhin Theorem. We propose the following candidate Lyapunov function

$$V(x, w) = x^T P x + \frac{a}{2} \int_0^\tau (1+s)w(s, t)^2 ds \quad (4.49)$$

where  $P = P^T > 0$  and control gains  $K$  and  $K_1$  are chosen such that they satisfy the linear matrix inequality (LMI)

$$\begin{bmatrix} P(A_d + B_d K) + (A_d + B_d K)^T P & P(A_{d1} + B_d K_1) \\ (A_{d1} + B_d K_1)^T P & -\alpha P \end{bmatrix} = -Q < 0 \quad (4.50)$$

for a chosen  $Q = Q^T > 0$  and some  $\alpha > 0$ , and the parameter  $a > 0$  is to be chosen later. The analysis first shows the exponential stability of the full state norm in the transform variable  $(\|X(t)\|^2 + \int_0^\tau w^2(s, t) ds)^{1/2}$ , and then uses that result to determine the stability of the full state norm in the control variable  $(\|X(t)\|^2 + \int_0^\tau v^2(s, t) ds)^{1/2}$ .

### Stability of the norm $(\|X(t)\|^2 + \int_0^\tau w^2(s, t) ds)^{1/2}$

To begin our analysis, we take the time derivative of the candidate Lyapunov function,  $V(x, w)$ . The derivative of the integral term can be taken as follows:

$$\begin{aligned} \frac{1}{2} \frac{d}{dt} \int_0^\tau (1+s)w(s, t)^2 ds &= \frac{1}{2} \int_0^\tau \frac{d}{dt} \left( (1+s)w(s, t)^2 \right) ds \\ &= \int_0^\tau w(s, t)w_t(s, t) ds + \int_0^\tau s w(s, t)w_t(s, t) ds \\ &= \int_0^\tau w(s, t)w_s(s, t) ds + \int_0^\tau s w(s, t)w_s(s, t) ds. \end{aligned} \quad (4.51)$$

The first integral term of this can be solved by substitution and the second integral can be solved by integration by parts. From this, we obtain

$$\frac{1}{2} \frac{d}{dt} \int_0^\tau (1+s)w(s,t)^2 ds = \frac{w(s,t)^2}{2} \Big|_0^\tau + \frac{sw(s,t)^2}{2} \Big|_0^\tau - \frac{1}{2} \int_0^\tau w(s,t)^2 ds \quad (4.52)$$

Since our control law was chosen such that  $w(\tau, t) = 0$ , we obtain

$$\frac{d}{dt} \int_0^\tau (1+s)w(s,t)^2 ds = -\frac{w(0,t)^2}{2} - \frac{1}{2} \int_0^\tau w(s,t)^2 ds. \quad (4.53)$$

With this result, taking the time-derivative of (4.49), we obtain

$$\begin{aligned} \dot{V} &= x^T((A_d + B_d K)^T P + P(A_d + B_d K))x \\ &\quad + x^T(t - \tau)((A_{d1} + B_d K_1)^T P + P(A_{d1} + B_d K_1))x(t - \tau) \\ &\quad + 2x^T P B_d w(0, t) - \frac{a}{2} w(0, t)^2 - \frac{a}{2} \int_0^\tau w(s, t)^2 ds. \end{aligned} \quad (4.54)$$

As per the conditions of the Razumikhin theorem, whenever the system trajectory  $x_t = x(t + \theta)$  for all  $-\tau \leq \theta \leq 0$  satisfies

$$V(x(t + \theta)) < pV(x(t)), \quad \forall \quad -\tau \leq \theta \leq 0 \quad (4.55)$$

for some  $p > 1$ , then we can conclude for any  $\alpha > 0$

$$\begin{aligned} \dot{V}(x, w) &\leq 2x^T P[(A_d + B_d K)x(t) + (A_{d1} + B_d K_1)x(t - \tau)] \\ &\quad + \alpha \left[ px^T(t)Px(t) - x^T(t - \tau)Px(t - \tau) \right] \\ &\quad + 2x^T(t)PB_d w(0, t) - \frac{a}{2} \|w(s, t)\|_2^2. \end{aligned} \quad (4.56)$$

Define the signal  $\phi_{0\tau}$  as

$$\phi_{0\tau} = \begin{pmatrix} x^T(t) & x^T(t - \tau) \end{pmatrix}^T. \quad (4.57)$$

Then, we see that this simplifies to

$$\begin{aligned} \dot{V} &\leq \phi_{0\tau}^T \begin{bmatrix} P(A_d + B_dK) + (A_d + B_dK)^T P & P(A_{d1} + B_dK_1) \\ (A_{d1} + B_dK_1)^T P & -\alpha P \end{bmatrix} \phi_{0\tau} \\ &+ 2x^T(t)PB_dw(0, t) - \frac{aw(0, t)^2}{2} - \frac{a\|w(s, t)\|_2^2}{2} \\ &= -\phi_{0\tau}Q\phi_{0\tau} + 2x^T(t)PB_dw(0, t) - \frac{aw(0, t)^2}{2} - \frac{a\|w(s, t)\|_2^2}{2}. \end{aligned} \quad (4.58)$$

Applying Young's inequality:

$$2x^T(t)PB_dw(0, t) \leq \frac{2\|x^T PB_d\|^2}{a} + \frac{aw(0, t)^2}{2} \quad (4.59)$$

which yields

$$\begin{aligned} \dot{V}(x, w) &\leq -\phi_{0\tau}Q\phi_{0\tau} + \frac{2}{a}\|x^T PB_d\|^2 - \frac{a\|w(s, t)\|_2^2}{2} \\ &\leq -\lambda_{\min}(Q)\|\phi_{0\tau}\|_2^2 + \frac{2}{a}\|PB_d\|^2\|x\|^2 - \frac{a\|w(s, t)\|_2^2}{2} \\ &\leq -\lambda_{\min}(Q)\|\phi_{0\tau}\|_2^2 + \frac{2}{a}\|PB_d\|^2\|\phi_{0\tau}\|^2 - \frac{a\|w(s, t)\|_2^2}{2} \\ &= -\frac{\lambda_{\min}(Q)}{2}\|\phi_{0\tau}\|^2 - \left(\frac{\lambda_{\min}(Q)}{2}\|\phi_{0\tau}\|^2 - \frac{2}{a}\|PB_d\|^2\|\phi_{0\tau}\|^2\right) - \frac{a}{2}\|w(x, t)\|^2, \end{aligned} \quad (4.60)$$

where  $\lambda_{\min}(Q)$  denotes the smallest eigenvalue of the matrix  $Q$ . Letting

$$a = \frac{4\lambda_{\max}(PB_dB_d^T P)}{\lambda_{\min}(Q)} \quad (4.61)$$

we obtain

$$\dot{V} \leq \frac{-\lambda_{\min}(Q)\|\phi_{0\tau}\|^2}{2} - \frac{2\lambda_{\max}(PB_dB_d^TP)}{\lambda_{\min}(Q)}\|w(s,t)\|^2. \quad (4.62)$$

Comparing this result with the candidate Lyapunov function given in (4.49), we see that

$$\dot{V} \leq -\min\left\{\frac{\lambda_{\min}(Q)}{2\lambda_{\max}(P)}, \frac{a}{2}\right\}V. \quad (4.63)$$

This result reveals that we have achieved exponential stability in terms of the full state norm in the transformed variable,  $(\|x(t)\|^2 + \int_0^\tau w(s,t)^2 ds)^{1/2}$ .

**Stability of the norm**  $(\|X(t)\|^2 + \int_0^\tau v^2(s,t) ds)^{1/2}$

To show exponential stability in terms of the full state norm in the control variable,  $(\|x(t)\|^2 + \int_0^\tau v(s,t)^2 ds)^{1/2}$ , we must obtain the inverse transform. This is done by solving the reverse problem, transforming from the target system (4.13)–(4.14) to the original system (4.11)–(4.12). This yields the inverse transformation

$$\begin{aligned} v(s,t) &= w(s,t) + \int_0^s K e^{\bar{A}_d(s-y)} B_d w(y,t) dy \\ &+ \int_0^s \left[ \left( K_1 e^{\bar{A}_d(s-y)} + K (e^{\bar{\Phi}_0(s-y)})_{12}^T \right) B_d w(s,t-\tau) \right] dy \\ &+ \int_0^s \left[ \left( K_1 e^{\bar{A}_d\sigma} + K (e^{\bar{\Phi}_0\sigma})_{12}^T \right) \bar{A}_{d1} x(t - (\sigma - s) - 2\tau) \right] d\sigma \\ &+ K e^{\bar{A}_d s} x(t) + \left( K_1 e^{\bar{A}_d s} + K (e^{\bar{\Phi}_0 s})_{12}^T \right) x(t - \tau) \end{aligned} \quad (4.64)$$

where  $\bar{A}_d = (A_d + B_d K)$ ,  $\bar{A}_{d1} = (A_{d1} + B_{d1} K_1)$ , and where  $\bar{\Phi}_0$  is given as

$$\bar{\Phi}_0 = \begin{bmatrix} \bar{A}_d & \bar{A}_{d1} \\ 0 & \bar{A}_d \end{bmatrix}. \quad (4.65)$$

Taking the integral of the square of the inverse transform we easily see that the first term and last two terms are exponentially stable. Using the Schwarz inequality, the remaining terms can be shown to satisfy

$$\int_0^D \left( \int_0^s K e^{\bar{A}_d(s-y)} B_d w(y, t) dy \right)^2 ds \leq \beta_1 \int_0^D w^2(s, t) ds \quad (4.66)$$

$$\int_0^D \left( \int_0^s \left[ \left( K_1 e^{\bar{A}_d(s-y)} + K (e^{\bar{\Phi}_0(s-y)})_{12}^T \right) B_d w(y, t - \tau) \right] dy \right)^2 ds \leq \beta_2 \int_0^D w^2(s, t) ds \quad (4.67)$$

$$\int_0^D \left( \int_0^s \left[ \left( K_1 e^{\bar{A}_d \sigma} + K (e^{\bar{\Phi}_0 \sigma})_{12}^T \right) \bar{A}_{d1} x(t - (\sigma - s) - 2\tau) \right] d\sigma \right)^2 ds \leq \beta_3 \|X(t)\|^2. \quad (4.68)$$

for some finite  $\beta_1, \beta_2, \beta_3 > 0$ . With this, we have shown the exponential stability of the full state norm  $(\|X(t)\|^2 + \int_0^D v^2(s, t) ds)^{1/2}$ .

## 4.4 Simulation Study

Similarly to the simulation study for the delay approximation case, we chose a set of parameters to demonstrate the capabilities of the designed controller. For comparison, we simulated the system against an ideal controller of the form

$$u(t) = Kx(t) + K_1 x(t - \tau). \quad (4.69)$$

This ideal controller is equivalent to the controller developed in the previous section when the actuator delay is assumed to be zero. The conditions and parameter values used in this simulation study are listed below:

- $g = 1, \eta = 1, \zeta = 0.5$
- $y_1(-r) = 1, y_2(-r) = -1, \tau \leq r \leq 0$

$$\bullet K = \begin{bmatrix} 0 & 2.0855 & 0 & 2.1971 \\ -2.9855 & 0 & -2.1971 & 0 \end{bmatrix}$$

$$\bullet K_1 = \begin{bmatrix} -0.2564 & 0 & -0.1941 & 0 \\ 0 & -0.2564 & 0 & -0.1941 \end{bmatrix}$$

The above gain matrices  $K$  and  $K_1$  were chosen as solutions to the linear matrix inequality given in (4.50). We conducted 2 sets of simulations, each with the parameters as listed above for  $\tau = 1$  and  $\tau = 3$ .

#### 4.4.1 Simulation Results

The first simulation that was conducted was done with the time delay  $\tau = 1$ . As can be seen in Fig. 4.1, this system is initially unstable for  $t < 1$  but is brought under control after this by the control inputs seen in Fig. 4.2. For comparison, Fig. 4.3 shows the states for the typical case without actuator delay compensation. From this, it is clear that the ideal controller is not able to provide satisfactory performance as the system goes unstable. Note that Fig. 4.2 displays the undelayed input  $u(t)$  and that this input was applied to the system at time  $t + \tau$ .

The  $\tau = 3$  case shows similar results, which is to be expected as, in the previous section, stability was shown to be independent of the delay and we are using the delay-independent criteria of the Razumikhin Theorem. Fig. 4.4 shows the outputs  $y_1, y_2$ . This figure also shows that our actuator delay compensation scheme was able to successfully stabilize and bring the trajectory back to the origin as opposed to the uncompensated state feedback case shown in Fig. 4.5. This verifies that our actuator delay compensation scheme and new backstepping transformation algorithm are capable of stabilization of systems with long actuator delays and state delays.

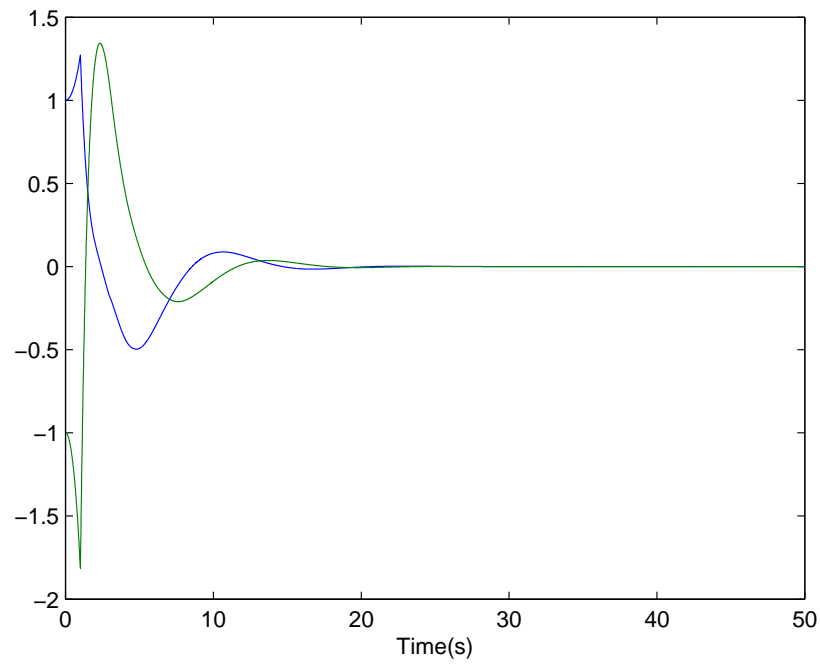


Figure 4.1: System outputs for  $\tau = 1$  case with actuator delay compensation.

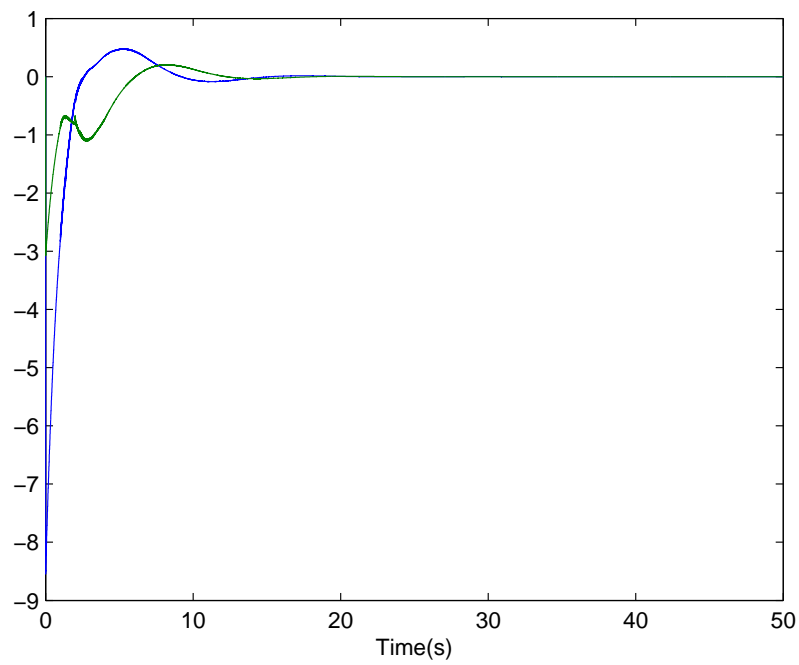


Figure 4.2: Control inputs  $u(t)$  for  $\tau = 1$  case with actuator delay compensation.

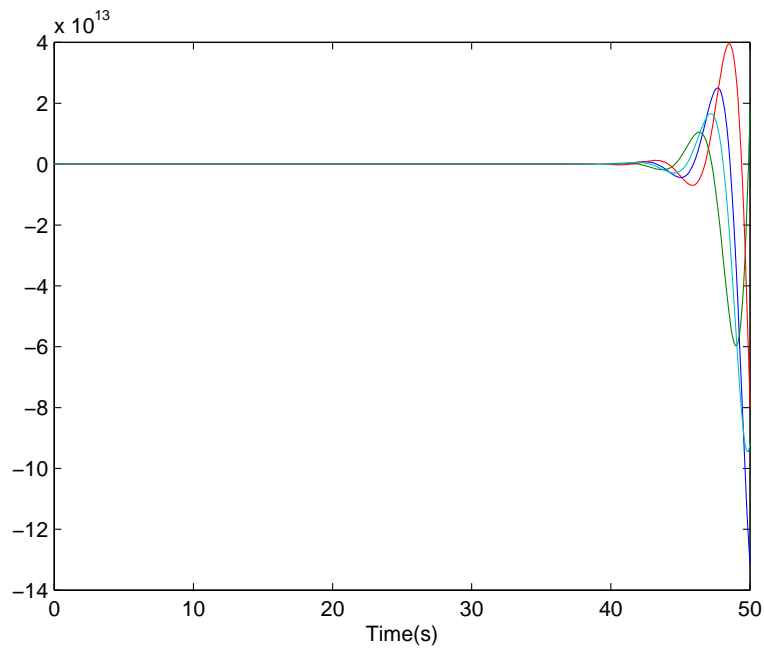


Figure 4.3: System states for  $\tau = 1$  case with ideal input (no compensation for actuator delay).

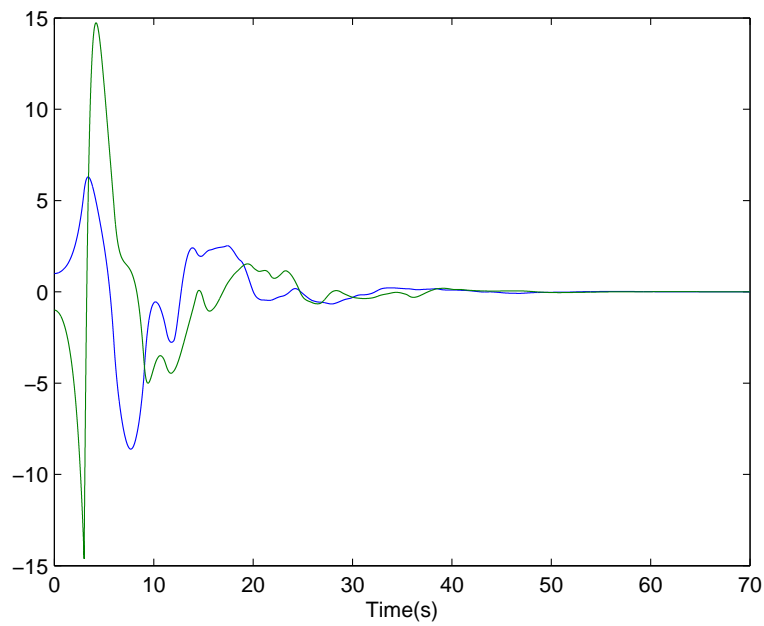


Figure 4.4: System outputs for  $\tau = 3$  case with actuator delay compensation

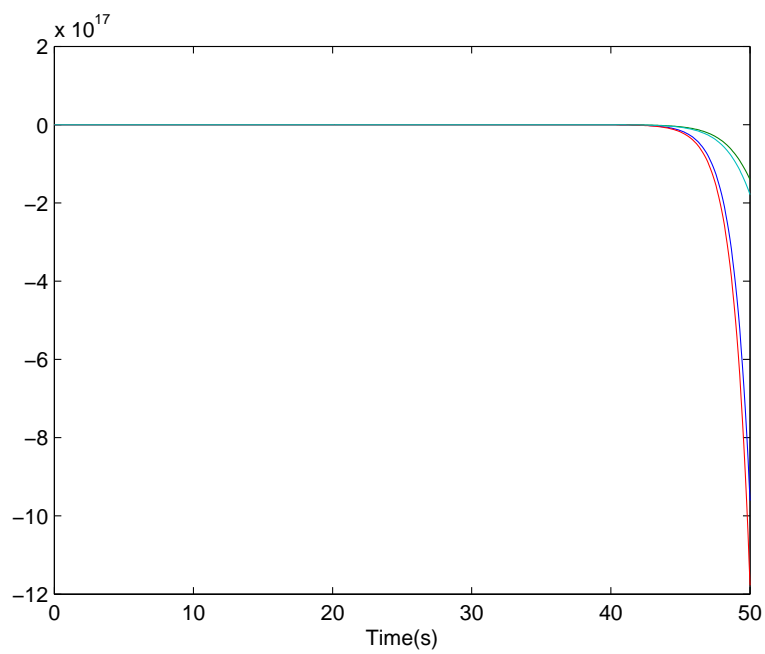


Figure 4.5: System states for  $\tau = 3$  case with ideal input (no compensation for actuator delay).

# Chapter 5

## Conclusions and Future Work

### 5.1 Conclusions

In this work, we have developed a robust indirect adaptive control scheme to control the thermoacoustic coupling phenomenon for the case when all system parameters are unknown, including time delays. This was achieved via a Pade approximation for the time delay and the utilization of a reduced-order parameter estimator. Additionally, for cases when delay approximation introduces large modeling errors, we developed a new backstepping algorithm for use with systems with arbitrarily long delays in both the states and the actuators.

As shown in Chapter 3, our indirect adaptive control scheme has the ability to guarantee closed-loop stability of the thermoacoustic coupling phenomenon with no knowledge of the system parameters and time delays. We developed robust laws that can guarantee the existence of a solution for all time, making this a viable technique for implementation. The adaptive scheme was also demonstrated to maintain this result in the presence of bounded input noise. Then, in Chapter 4, the developed backstepping algorithm was shown to result in stability of the full state norm in the presence of arbitrarily long time delays when all system parameters are known. This result was found for a general class of linear systems that have both input and state

delays. The thermoacoustic coupling model given in (2.40) falls into this class of systems, so this technique is also viable for control of this phenomenon, particularly when the use of a Pade approximation introduces large modeling errors.

## 5.2 Future Work

There is a large amount of potential for advancement of the research and studies done in this thesis. For the work done in Chapter 3, we assume that the simplified model gives a sufficient representation of the physical distributed system. For this work to be entirely validated through simulation, it is necessary to simulate against the unsimplified thermoacoustic models given in [2]. Additionally, fault tolerant techniques could be examined for the case when some of the fuel injectors are susceptible to a variety of failures. Similar controller design techniques may be applicable to other processes that adhere to the general model specified in (2.39).

Chapter 4 presents only the beginning of the work that is able to be done with the developed backstepping algorithm. This algorithm is a modification of that presented in [17], which was shown to be compatible with adaptive parameter estimation schemes where the time delay was able to be adaptively estimated, as demonstrated in [19],[20],[21]. Additionally, modifying techniques given in [19] would allow for the design of an adaptive parameter estimator for the unknown system parameters. Application of robust techniques could then be used to ensure stabilization of the system and the adaptive estimates in the presence of bounded noise and other disturbances.

# Bibliography

- [1] M. Krstic and A. Banaszuk, “Multivariable adaptive control of instabilities arising in jet engines,” *Control Engineer Practice*, vol. 14, pp. 833-842, July 2006.
- [2] A. Banaszuk, G. Hagen, P. Mehta, J. Ooppelstrup, “A linear model for control of thermoacoustic instabilities on an annular domain,” *Proceedings of the IEEE Conference on decision and control*, Maui, HI, 2003, pp. 2346-2351.
- [3] Y. Ling and G. Tao, “Adaptive backstepping control design for linear multivariable plants,” *International Journal of Control*, vol. 68, no. 6, pp. 1289-1304, 1997.
- [4] G. Tao, *Adaptive Control Design and Analysis*, Wiley, Hoboken, NJ, 2003.
- [5] P. A. Ioannou, and J. Sun, *Robust Adaptive Control*, Prentice-Hall, Englewood Cliffs, NJ, 1996.
- [6] G. Franklin, J. Powell, and A. Emami-Naeini, *Feedback Control of Dynamic Systems*, Prentice-Hall, Upper Saddle River, NJ, 2010.
- [7] A.M. Annaswamy and A.F. Ghoniem, “Active control of combustion instability: Theory and practice,” *IEEE Control Systems Magazine*, December 2002.
- [8] M. Fleifil, J.P. Hathout, A.M. Annaswamy, and A.F. Ghoneim, “The origin of secondary peaks with active control of thermoacoustic instability,” *Combustion Science and Technology*, vol. 133, no. 4-6, pp. 227-265, 1998.

- [9] Y.C. Chu, A.P. Dowling, and K. Glover, "Robust control of combustion oscillations," *Proceedings of the Conference on Control Applications*, Trieste, Italy, August 1998.
- [10] G. Billoud, M.A. Galland, C. Huynh Huu, and S. Candel, "Adaptive active control of combustion instabilities," *Combustion Science and Technology*, vol. 164, no. 4-6, pp. 65-94, January 1992.
- [11] M. Krstic, A.S. Krupadanam, and C. Jacobson, "Self-tuning control of a nonlinear model of combustion instabilities," *IEEE Control System Technology*, vol. 7, no. 4, pp. 424-436, July 1999.
- [12] A.M. Annaswamy, M. Fleifil, J. Rumsey, J.P. Hathout, R. Prasanth, and A.F. Ghoniem, "Thermoacoustic instability: Model-based optimal control designs and experimental validation," *IEEE Transactions on Control Systems Technology*, vol. 8, no. 6, pp. 905-918, November 2000.
- [13] K. Yu, K.J. Wilson, and K.C. Schadow, "Scale-up experiments on liquid-fueled active combustion control," *34th AIAA/ASME/SAE/ASEE Joint Propulsion Conference*, AIAA 98-3211, Cleveland, OH, 1998.
- [14] S.S. Sattinger, Y. Neumeier, A. Nabi, B.T. Zinn, D.J. Amos, and D.D. Darling, "Sub-scale demonstration of the active feedback control of gas-turbine combustion instabilities," *ASME Journal of Engineering for Gas Turbines and Power*, vol. 122, no. 2, pp. 262-268, January 2000.
- [15] J. Hermann, A. Orthmann, S. Hoffmann, and P. Berenbrink, "Combination of active instability control and passive measures to prevent combustion instabilities in a 260 mw heavy duty gas turbine," *NATO RTO/AVT Symposium on Active*

- Control Technology for Enhanced Performance in Land, Air, and Sea Vehicles*, Braunschweig, Germany, May 2000.
- [16] S. Garg, “Aircraft Turbine Engine Control Research at NASA Glenn Research Center,” *Journal of Aerospace Engineering*, vol. 26, no. 2, pp. 422-438, April 2013.
- [17] M. Krstic and A. Smyshlyaev, “Backstepping boundary control for first order hyperbolic PDEs and application to systems with actuator and sensor delays,” *Systems and Control Letters*, vol. 57, no. 9, pp. 750-758, April 2008.
- [18] A. Smyshlyaev and M. Krstic, “Closed form boundary state feedbacks for a class of 1D partial integro-differential equations,” *IEEE Transactions on Automatic Control*, vol. 49, no. 12, pp. 2185-2202, December 2004.
- [19] D. Bresch-Pietri and M. Krstic, “Adaptive trajectory tracking despite unknown input delay and plant parameters,” *Automatica*, vol. 45, no. 9, pp. 2074-2081, June 2009.
- [20] D. Bresch-Pietri and M. Krstic, “Delay-Adaptive predictor feedback for systems with unknown long actuator delay,” *IEEE Transactions on Automatic Control*, vol. 55, no. 9, pp. 2106-2112, September 2010.
- [21] D. Bresch-Pietri and M. Krstic, “Delay-adaptive control for nonlinear systems,” *IEEE Transactions on Automatic Control*, vol. 59, no. 5, pp. 1203-1218, May 2014.
- [22] C. Van Loan, “Computing Integrals Involving the Matrix Exponential,” *IEEE Transactions on Automatic Control*, vol. 23, no. 3, pp. 395-404, June 1978.
- [23] F. Carbonell, J. C. Jimenez, and L. M. Pedroso, “Computing multiple integrals involving matrix exponentials,” *Journal of Computational and Applied Mathematics*, vol. 213, pp. 300-305, March 2008.

- [24] S. Garg, P. J. Ouzts, C. F. Lorenzo, and D. L. Mattern, "IMPAC - an integrated methodology for propulsion and airframe control," *Proceedings of the 1991 American Control Conference*, Boston, MA, 1991.
- [25] S. Garg and D. L. Mattern, "Application of an integrated methodology for propulsion and airframe control design to a STOVL aircraft," 94-3611, AIAA, Reston, VA, 1994.
- [26] M. M. Bright, et. al., "Piloted evaluation of an integrated methodology for propulsion and airframe control design," 94-3612, AIAA, Reston, VA, 1991.
- [27] T. Guo, P. Chen, and L. Jaw, "Intelligent life-extending controls for aircraft engines", 2004-6468, AIAA, Reston, VA, 2004.
- [28] L. Jaw and J. Mattingly, *Aircraft engine controls design, system analysis, and health monitoring*, AIAA, Inc., Reston, VA, 2009.
- [29] B. Pourbabaee, N. Meskin, and K. Khorasani, "Multiple-Model Based Sensor Fault Diagnosis using Hybrid Kalman Filter Approach for Nonlinear Gas Turbine Engines," *Proceedings of the 2013 American Control Conference*, Washington, DC, 2013, pp. 4724-4730.
- [30] N. Daroogheh, N. Meskin, and K. Khorasani, "Particle Filtering for State and Parameter Estimation in Gas Turbine Engine Fault Diagnostics", *Proceedings of the 2013 American Control Conference*, Washington, DC, 2013, pp. 4349-4355.
- [31] M. Lichtsinder and Y. Levy, "Jet Engine Model for Control and Real-Time Simulations," *Journal of Engineering for Gas Turbines and Power*, vol. 128, no. 4, pp. 745-753, May 2003.

- [32] K. Parker and T. Guo, "Development of a turbofan engine simulation in a graphical simulation environment," TM-2003-21243, NASA, Cleveland, OH, <http://ntrs.nasa.gov/>.
- [33] J. A. DeCastro, J. S. Litt, and D. K. Frederick, "A modular aero-propulsion system simulation of large commercial aircraft engine," 2008-4579, AIAA, Reston, VA, 2008.
- [34] R.D. May, et al., "A high fidelity simulation of a generic commercial aircraft engine and controller," *AIAA/ASME/SAE/ASEE Joint Propulsion Conference*, Nashville, TN, 2010.
- [35] Environmental Protection Agency, "Nitrogen Dioxide: Air Emissions Sources," Internet: [www.epa.gov/oaqps001/nitrogenoxides/](http://www.epa.gov/oaqps001/nitrogenoxides/), Aug. 15, 2014, [Mar. 18, 2015].
- [36] Environmental Protection Agency, "Regulatory Announcement: New Emission Standards for New Commercial Aircraft Engines," Internet: [www.epa.gov/otaq/regs/nonroad/aviation/420f05015.pdf](http://www.epa.gov/otaq/regs/nonroad/aviation/420f05015.pdf), Nov. 2005, [Mar. 18, 2015].
- [37] Environmental Protection Agency, "Aircraft," Internet: [www.epa.gov/otaq/aviation.htm](http://www.epa.gov/otaq/aviation.htm), Mar. 13, 2015, [Mar. 18, 2015].
- [38] Airplane Flying Handbook, *Basic components of a gas turbine engine*. 2004.
- [39] O. Smith, "A controller to overcome dead time," *Indian Scientist Association in Japan*, vol. 6, pp. 28–33, 1957.
- [40] A. Manitius and A. Olbrot, "Finite spectrum assignment for systems with delays," *IEEE Transactions on Automatic Control*, vol. 24, no. 4, pp. 541-552, August 1979.

- 
- [41] W.H. Kwon and A.E. Pearson, “Feedback stabilization of linear systems with delayed control,” *IEEE Transactions on Automatic Control* vol. 25, no. 2, pp. 266–269, April 1980.
- [42] Z. Artstein, “Linear systems with delayed controls: A reduction,” *IEEE Transactions on Automatic Control*, vol. 27, no. 4, pp. 869–879, August 1982.
- [43] G. Kulikov and H. Thompson, *Dynamic Modelling of Gas Turbines: Identification, Simulation, Condition Monitoring, and Optimal Control*, Springer, London, 2004.
- [44] K. Gu, V. Kharitonov, and J. Chen, *Stability of Time-Delay Systems*, Birkhauser, Boston, MA, 2003.